Item No 830-H-15

NAS 1.60:1840

NASA Technical Paper 1840

COMPLETED

ORIGINAL

Design and Analysis of a Torsion Braid Pendulum Displacement Transducer

Emanuel Rind and Emmett L. Bryant

JUNE 1981

NASA

NASA Technical Paper 1840

Design and Analysis of a Torsion Braid Pendulum Displacement Transducer

Emanuel Rind and Emmett L. Bryant
Langley Research Center
Hampton, Virginia

National Aeronautics
and Space Administration

**Scientific and Technical
Information Branch**

1981

I

Blank Page

SUMMARY

The dynamic properties at various temperatures of braids impregnated with polymer can be measured by using the braid as the suspension of a torsion pendulum. This report describes the electronic and mechanical design of a torsional braid pendulum displacement transducer which is an advance in the state of the art. The transducer uses a unique optical design consisting of refracting quartz windows used in conjunction with a differential photocell to produce a null signal. The release mechanism for initiating free torsional oscillation of the pendulum has also been improved. Analysis of the precision and accuracy of the transducer indicated that the maximum relative error in measuring torsional amplitude was approximately 0.7 percent. A serious problem inherent in all instruments which use a torsional suspension was analyzed: misalignment of the physical and torsional axes of the torsional member which results in modulation of the amplitude of the free oscillation.

INTRODUCTION

Torsional braid pendulum displacement transducers have been used to generate the dynamic mechanical spectra of polymeric materials over a wide temperature range (refs. 1 and 2). Previously, a solid polymeric suspension element was part of the torsion pendulum, but because of undesirable effects due mostly to temperature changes, the element was changed to a multifilament glass braid impregnated with the polymer sample to be studied. Tests have shown that this braid makes the undesirable temperature effects insignificant. With the impregnated braid suspension mounted in a furnace tube so that its temperature can be controlled, the pendulum is released from an initial torsional offset which initiates free torsional oscillation. Ideally, the pendulum motion should have a damped sinusoidal waveform from which the damping coefficient, rigidity, and shear modulus of the polymer-impregnated braid can be obtained. Since this information is very useful for practical application of various polymers and since the braid-suspended pendulum system has decided advantages over other methods for obtaining this information, considerable effort has been and is still being expended to improve transducers and obtain real-time data analysis capability (refs. 3, 4, and 5). The existing pendulum displacement transducer used to measure the pendulum oscillation is described in reference 1. A fixed and a moving polarizer are attached to the pendulum, and a light beam is passed through both into a photomultiplier tube. The output of the tube is a function of pendulum displacement. A less bulky, simpler to operate, and more sensitive transducer was desired with a better method for initiating the free torsional oscillation. The ensuing research effort resulted in a torsional braid pendulum transducer which meets and exceeds these criteria and which is considered an advance in the state of the art. The transducer uses a unique optical system for which a patent has been awarded (ref. 6). It employs a differential photocell which was made at Langley Research Center, since it could not be obtained commercially. These and other innovations are described in this paper. A

complete mathematical analysis was also made of the transducer precision and accuracy. The transducer, the innovations used in its design, and the results of the mathematical analysis are applicable to similar areas of endeavor.

SYMBOLS

a	$= c\omega/\omega'$ (see eq. (C20))
b	$= \ell/2J$
c	damping coefficient of torsional member
$c_1, c_2, \ldots$	constants
D	inside diameter of coil
d	window thickness; also diameter of coil wire; also translation of θ to θ'
$d_1, d_2, \ldots$	constants
G	shear modulus
I	mass moment of inertia
J	torsional polar moment of inertia
J_A	polar areal moment of inertia of the torsional member
K	torsional spring constant or torsional rigidity
L	length of torsional member
L_1, L_2	lengths of two parts of compound torsional member
$\mathfrak{L}$	Lagrangian function
l	length of coil
ℓ	damping constant
m	displacement in figure 10; also mass of pendulum
N	number of layers of wire in coil
n	displacement in figure 10; also refractive index; also number of half-periods between peak amplitudes

n_1	fractional overshoot
R	radius of curvature of window
S	total length of wire in coil
T	period of torsional oscillation; also kinetic energy
T_N	component of T_Y normal to torsional member
T_Y	unperturbed torsion in torsional member
$T_{\|\|}$	component of T_Y parallel to torsional member
t	time
V	potential energy
x,y,z	coordinates of center of gravity of pendulum
δ	phase angle
ζ	angle between incoming ray and normal to curved surface of window
η	angle between plane surface of window and exiting refracted ray
θ	torsional displacement of pendulum
θ_o	initial torsional displacement of pendulum
θ'	θ measured from reference datum other than $\theta = 0$
ξ	angle between refracted ray and normal to curved surface of window
σ	standard deviation of mean value
Φ	angular displacement of window
ϕ,ψ	angular displacements of torsional member from Y-axis
ω	natural angular velocity
ω'	damped angular velocity

A dot over a symbol denotes differentiation with respect to time.

DESCRIPTION OF TRANSDUCER

The torsional braid pendulum displacement transducer with its related hardware and electronics is shown in figure 1. Figure 2 is a cutaway drawing

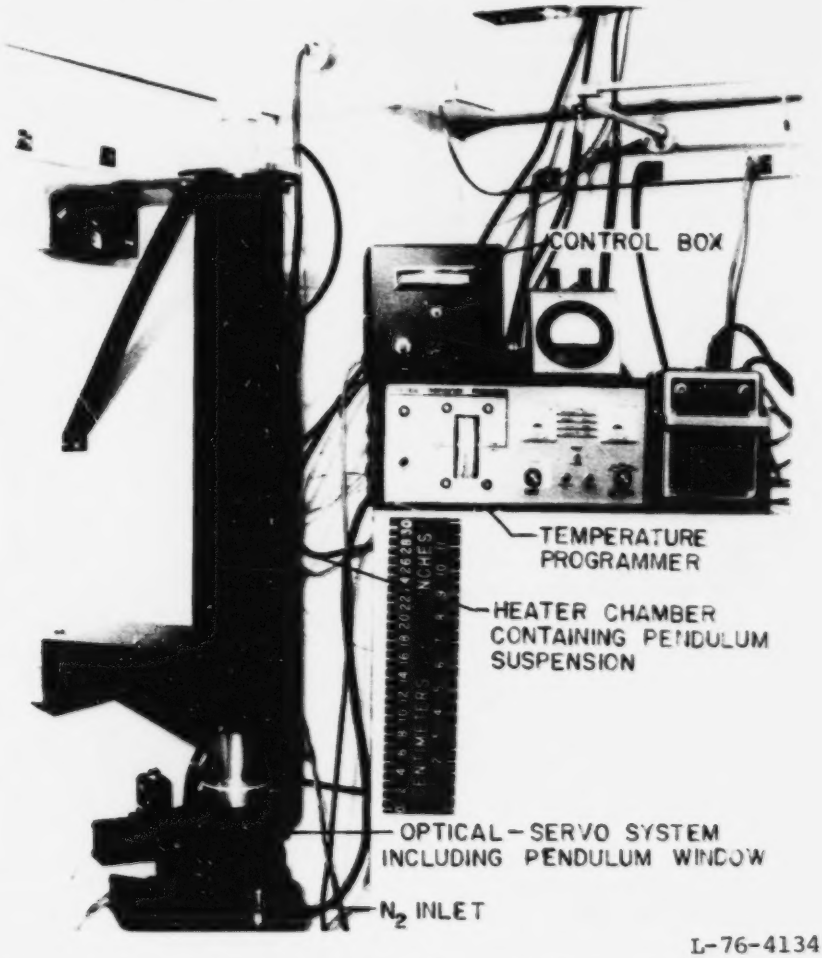

Figure 1.- Torsional braid pendulum displacement transducer installed with related hardware and electronics.

of the mechanical-optical part of the transducer which more clearly shows its operation. Light transmitted from the source (14) through a servo-driven window (16) is collimated (18), passed through a focusing lens (11) and through a second window (24) mounted on the torsional braid pendulum, and brought to focus on a differential photocell (26). As the pendulum rotates, the motion of the light source image on the photocell produces an error signal which is fed into an electronic circuit which drives the galvanometer (13) and its window (16) in a direction that restores the light image to its original, or null,

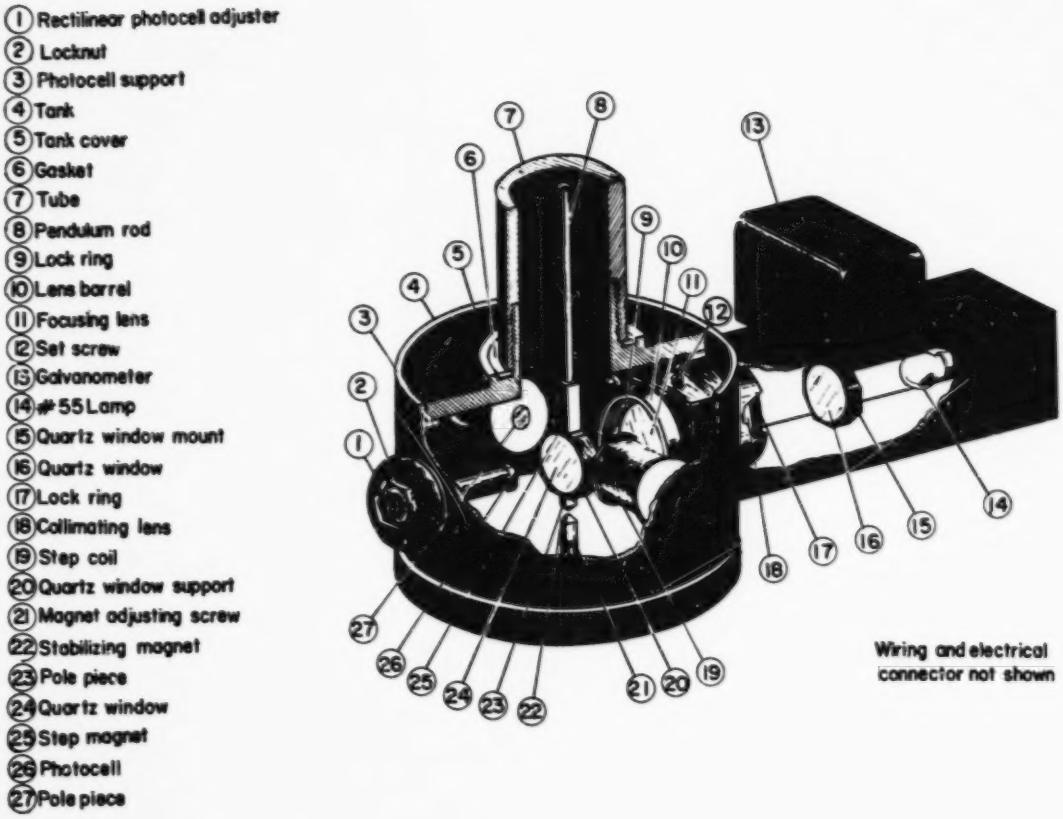

Figure 2.- Mechanical-optical part of torsional braid pendulum displacement transducer.

position. The current that drives the galvanometer is proportional to the pendulum displacement and is taken as the output of the transducer.

In figure 2 the light source (14) can be placed so that its filament is vertical. With power off, the galvanometer window (16) is at right angles to the optical axis. The lens (18) collimates the light source. The focusing lens (11) was chosen so that the light beam covers less than half the diameter of the second window (24). The light beam is brought to focus on the photocell (26) by moving the photocell support (3) in or out. The pendulum is made long enough so that the window suspended from it is approximately centered with the optical axis. Initially, the pendulum window is perpendicular to the optical axis, and the small permanent magnet (25) is aligned parallel to the optical axis and perpendicular to the field produced by the step coils (19) and (27). When energized, the coils give the pendulum an initial angular offset. Deenergizing the coils allows the pendulum to freely oscillate. When this occurs, the focused lamp filament image starts to move across the differential photocell (26) producing an error signal. This signal is fed into an electronic circuit which drives the galvanometer in the same direction as that of the pendulum

window to cause the light spot to remain at nearly the null position on the photocell. (The galvanometer moves in the same direction as the pendulum window because of image reversal through the lenses.) With a symmetrical optical system, the galvanometer tracks the pendulum in a one-to-one ratio. A voltage proportional to the current driving the galvanometer is the transducer output.

Figure 3 is a schematic of the electrical circuit. The filament supply on the lamp is voltage regulated below its rated value to maintain the filament at a fixed operating condition and to give it long life. The manual step switch energizes the coils which produce the initial torsional displacement of the pendulum. However, over a wide range of braid torsional stiffness, a change in the permanent magnet may be necessary to obtain the desired angular offset. The step B input is for remotely initiating the pendulum oscillation.

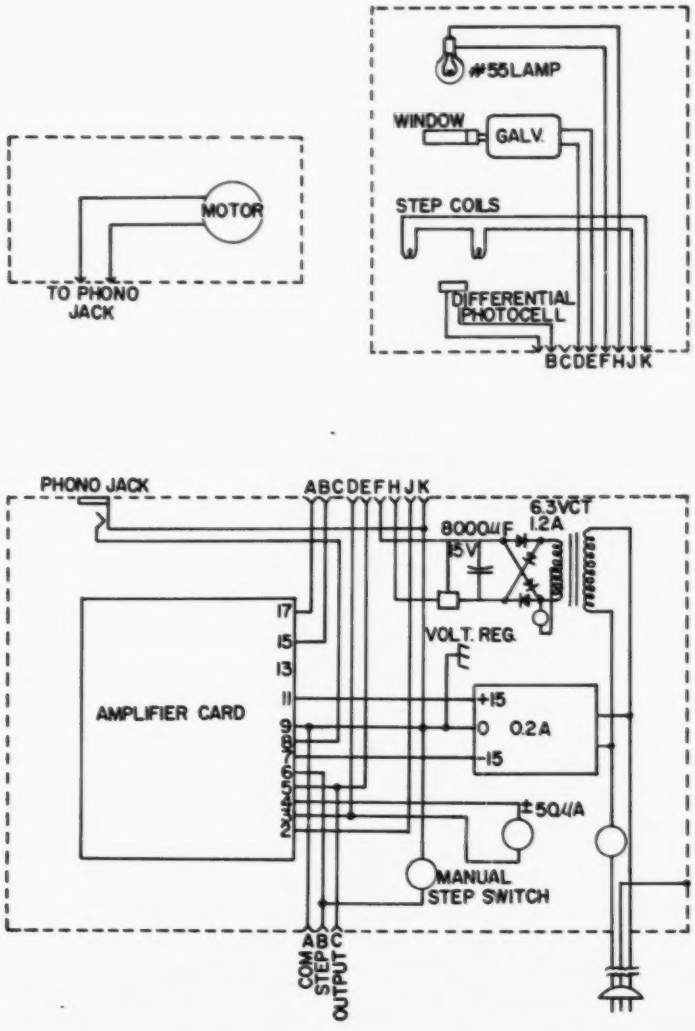

Figure 3.- Overall wiring diagram.

Figure 4 is the wiring diagram for the electronic circuit. The error signal from the photocell is fed into operational amplifier A1. Circuit gain is

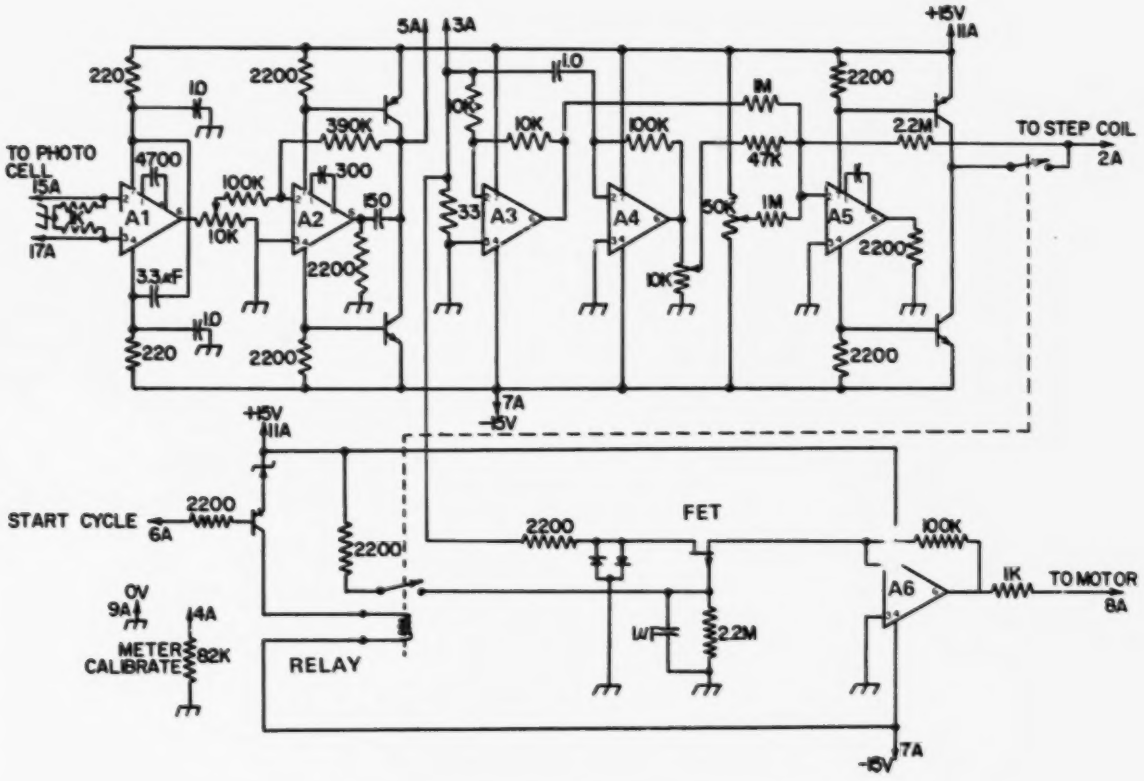

Figure 4.- Wiring diagram of the electronic circuit.

controlled by the 10-kΩ potentiometer which is adjusted to give the maximum gain with acceptable stability. From there, the signal goes to amplifier A2 which is coupled to two transistors. Together these act as a power amplifier supplying the galvanometer. The remainder of the circuit, to the right of the 3A line and below the dotted line, is essentially concerned with the mechanism for initiating the angular offset and with the motor control for maintaining the average position of the pendulum.

The current flowing to the galvanometer is directly proportional to the pendulum displacement. A voltage which is obtained linearly from the galvanometer current is fed into amplifier A3, into amplifier A4, and into the motor circuit. Amplifier A3 receives a signal which is proportional to the pendulum position and inverts its phase 180° without gain. Amplifier A4 needs only the ac component of the signal since it is a differentiator whose output is proportional to the pendulum angular velocity. Its output is phase shifted 90° and provides damping when these signals are summed at the input to amplifier A5. This damping only acts when the step coil is energized and is used to damp out

any oscillations in the initial offset. The 10-kΩ potentiometer associated with it gives damping control. The 50-kΩ potentiometer biases the direction in which the pendulum will be offset and acts as an adjustment to obtain a desired initial offset. Amplifier A5, in conjunction with its transistors, acts as a power amplifier supplying the coil.

A motor system, to which the pendulum is mounted, offers a method of maintaining the average pendulum position. This is accomplished as follows. When the contacts are open (that is, the relay and step coils are not energized), the motor maintains the pendulum at its average null position. The response of the motor is so slow that it does not respond to the normal oscillations of the pendulum. When the coil and relay circuit is open, the field effect transistor (FET) acts as a low resistance, and amplifier A6 drives the motor. The motor operates at a low power requiring 12 volts and 2 mA. Then a switch closure or TTL (transistor-transistor logic) logical zero is applied across pin 6A to the ground; this closes the relay which energizes the step coils and biases the FET to a large resistance state. This inhibits further motor operation. The step coil, however, is now energized and its field acting on the permanent magnet on the pendulum causes the pendulum to displace through a specified angle. This specified displacement is obtained by summing three signals at the negative input of amplifier A5. These signals are obtained from the 50-kΩ potentiometer, from the actual displacement of the galvanometer, and from the angular velocity of the galvanometer (controlled through a 10-kΩ potentiometer) which provides damping in the step mode of operation.

The two diodes across the gate and the drain of the FET limit the voltage to a maximum of about 0.5 volt. This keeps the FET resistance within a reasonably linear range.

DESIGN CONSIDERATIONS

In this section, design considerations are described which led to this particular design of the torsional braid pendulum displacement transducer. Important requirements for the light source are that the part of the filament forming the image on the photocell lie in a plane, that its position not shift, that it have long life, and that it have a constant intensity to prevent an apparent image displacement because of filament inhomogeneities or filament stress distortion. An incandescent filament lamp with a voltage regulator supplying a stable, underrated lamp voltage fulfilled these needs.

The next consideration is the lens and window optics. If the system is nonsymmetric, that is, unequal image and object distances, the two windows have different sensitivities in generating the beam displacement. This may be desirable when the range of swing desired from the pendulum has to be different from that of the tracking sensor. However, the combined distance of object and image is minimum when they are equal. Shorter focal length lenses, for a given diameter, collect more light and result in a more compact design. However, as the focal length becomes shorter, the refractor window causes more broadening of the line source, in the focal plane. This broadening does not cause any problems, since the photocell responds to the average intensity value.

For much more control and ease of setup, a two-lens system, with one acting as a collimator, was chosen. Since the optics preclude placing the refractor windows in the collimator space between the lenses, one window is placed in the object space and the other in the image space. Their placement is not critical provided that they always pass the entire beam. A typical symmetrical setup of an optical system showing image broadening and displacement of the image by the refractor window is shown in figure 5.

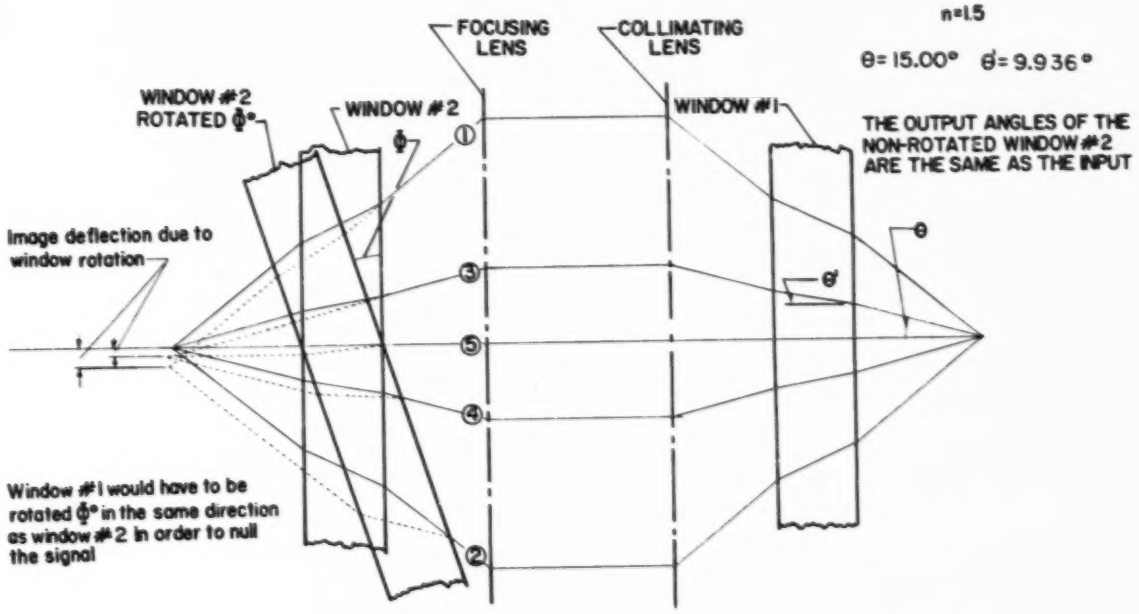
FOCUSING LENS
COLLIMATING LENS
n=1.5
θ=15.00° θ'=9.936°
WINDOW #2 ROTATED Φ°
WINDOW #2
WINDOW #1
THE OUTPUT ANGLES OF THE NON-ROTATED WINDOW #2 ARE THE SAME AS THE INPUT
Image deflection due to window rotation
θ
θ'
Window #1 would have to be rotated Φ° in the same direction as window #2 in order to null the signal

Figure 5.- A symmetric, collimated optical system showing image formation through quartz windows.

Since a differential photocell was not available commercially, a standard photocell was altered as shown in figure 6. It generates a differential voltage at its terminals, which when fed to a differential amplifier results in an output proportional to the light displacement from the null position on the photocell. Reference 7 discusses the theory of the differential photocell.

The coils causing the field that produces the initial offset of the pendulum are connected in series. The main consideration here is to limit the current they draw from the power supply to a reasonable value. Since the handbooks do not supply this coil design information, the formula is derived in appendix A, with an example of its use. The coils react with a permanent magnet, located on the bottom of the pendulum, to produce the initial offset. It is important that this offset be repeatable so that the data reduction is made for the same initial amplitude. This may be quite important if the damping coefficient is not constant. Constant offset amplitude is provided over an extreme range of braid rigidities by using three different strength permanent magnets and electrically changing the coil field strength.

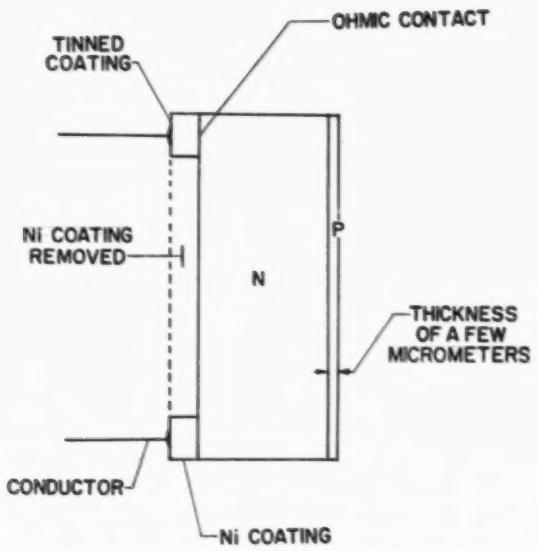

Figure 6.- Drawing of a standard photocell showing alterations which make it a differential photocell.

A high torque galvanometer with good linearity and minimal hysteresis is required, and one was obtained that met these criteria.

Since the magnetic fields associated with the galvanometer and pendulum magnet may interact and cause instability, the tank (fig. 2) was made of soft iron to act as a magnetic shield. It was also designed so that the gas for heating the braid was baffled so as not to disturb the pendulum. A magnetic stabilizer was also added to the pendulum to minimize perturbations which were discovered after the transducer was designed. After the source of the perturbations was finally isolated, the cause and effects of this problem were analyzed and are discussed in appendix B.

In a damped dynamic system, the response is a function of the forcing frequency, the natural frequency of the system, and the damping. Generally, it is desired that the transducer follow the system oscillation as exactly as possible, that is, in phase, with equal or proportional amplitudes. The forcing function is the pendulum motion with frequency of about 1 Hz and an exponentially modulated amplitude. (Since an exponential input results in a constant input-output amplitude ratio and a constant phase shift, the pendulum over short time intervals and in the damping range of interest is essentially acting as a sine wave input to the tracker transducer system.) A response curve for a sinusoidal forcing function is shown in figure 7. Clearly, the flattest response is obtained for a damping coefficient of 0.707. This damping also gives the best phase shift characteristics, but this consideration is relatively unimportant since the natural frequency of the transducer which is essentially that of the galvanometer (about 76 Hz) is much greater than the forcing frequency (1 Hz) and very little phase shift occurs. Also, at this forcing frequency, there is considerable latitude in choosing a damping coefficient that gives a relatively flat response.

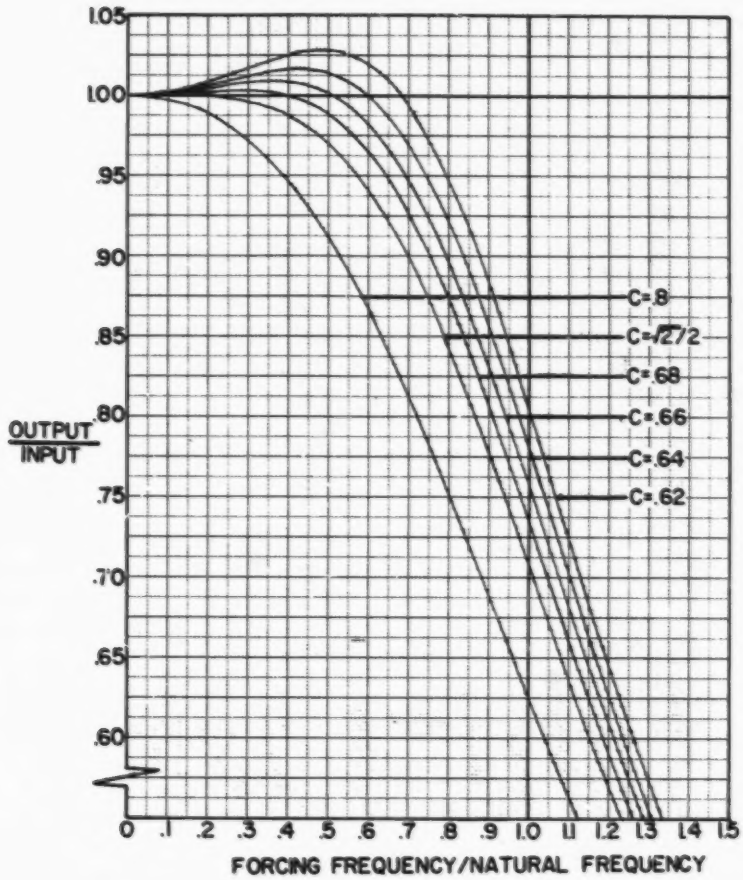

Figure 7.- Dynamic response curves for a damped, second order system with a sinusoidal forcing function.

Hence, the system stability is considered more critical. In a closed loop system, high gain is desirable. However, as the gain increases, the effective damping decreases and a condition of instability may occur. The circuit stability can be investigated by obtaining the open loop gain versus frequency or phase angle versus frequency. For a control system with a second order characteristic, response peaking occurs at the damped natural frequency f_d and a 90^o phase shift occurs at the natural frequency f_n. From this point the gain rolloff approaches -12 dB/octave. If, in the open loop, the gain is greater than or equal to 1 when a 180^o phase shift occurs, the closed loop circuit is unstable. A check of the response of the original circuit (fig. 8) showed that it was unstable. In order to maintain high gain and stability, the circuit was altered to use velocity feedback to stabilize the circuit. This approach was unsuccessful; thus the circuit was modified to resemble a first order system in its operational range, which has a -6 dB/octave gain rolloff, does not peak on the gain, and theoretically has a 90^o phase shift at infinity. The frequency response of this system, shown in figure 9, is stable.

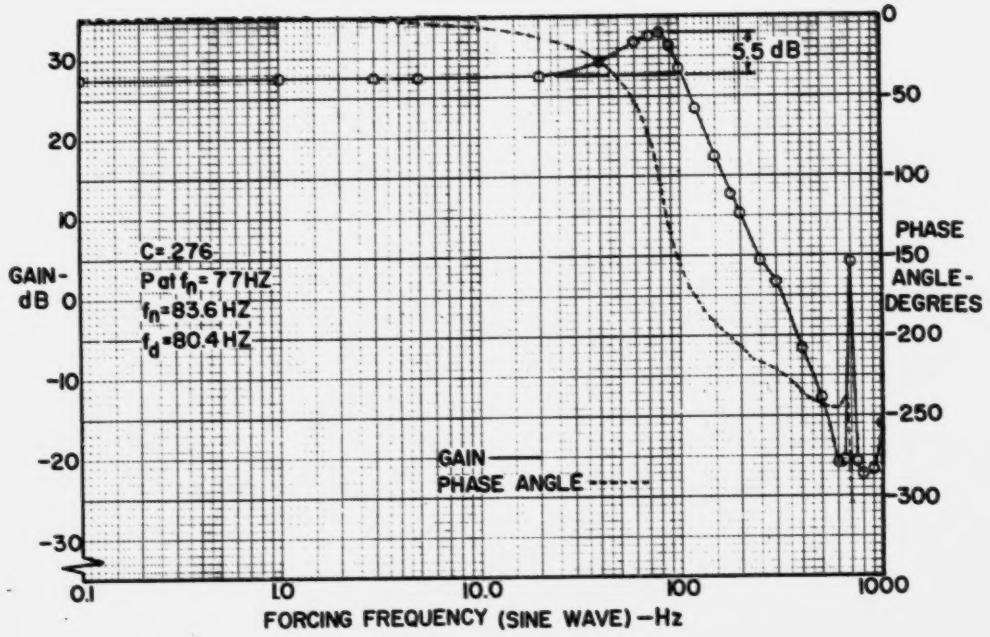

Figure 8.- Open loop frequency response characteristics of the original second order system.

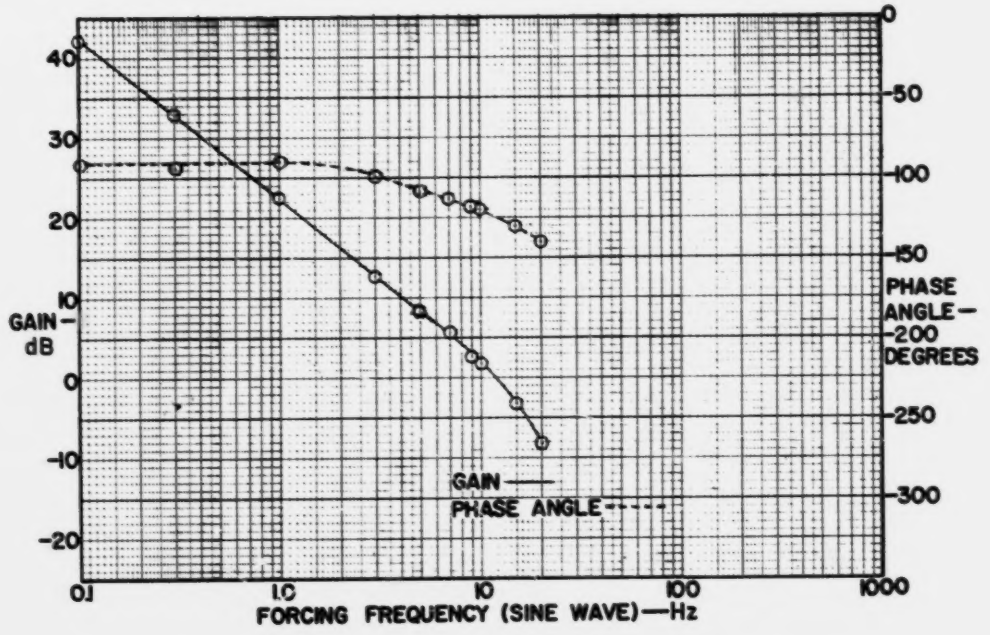

Figure 9.- Open loop frequency response characteristics of the final, first order system.

PRECISION

Factors affecting precision are, first, those elements which cause a nonlinear output response for a given input and, second, the errors introduced in the data reduction. As was mentioned, the errors from the light source were minimized and these errors together with those from the lens system are inconsequential.

To determine what error is introduced by window curvature (nonparallelism of the window faces), a calculation was made to see what curvature would produce an error of 1 percent of full scale. Full-scale angular displacement of the pendulum is $\pm 15^{\circ}$. For an incidence angle of 15°, the angle of refraction through a window with refractive index of 1.5 is 9.936°, as shown in figure 5. Thus, the full-scale displacement of the light image caused by window refraction is ($d \tan 15^{\circ} - d \tan 9.936^{\circ}$) where d, the window thickness, is 0.635 cm. Therefore, the full-scale displacement is 0.0589 cm, and the 1-percent full-scale error is 5.891×10^{-4} cm.

Figure 10 shows dimensions of the optical system for which the calculation of error due to window curvature was made. All the curvature was assumed on

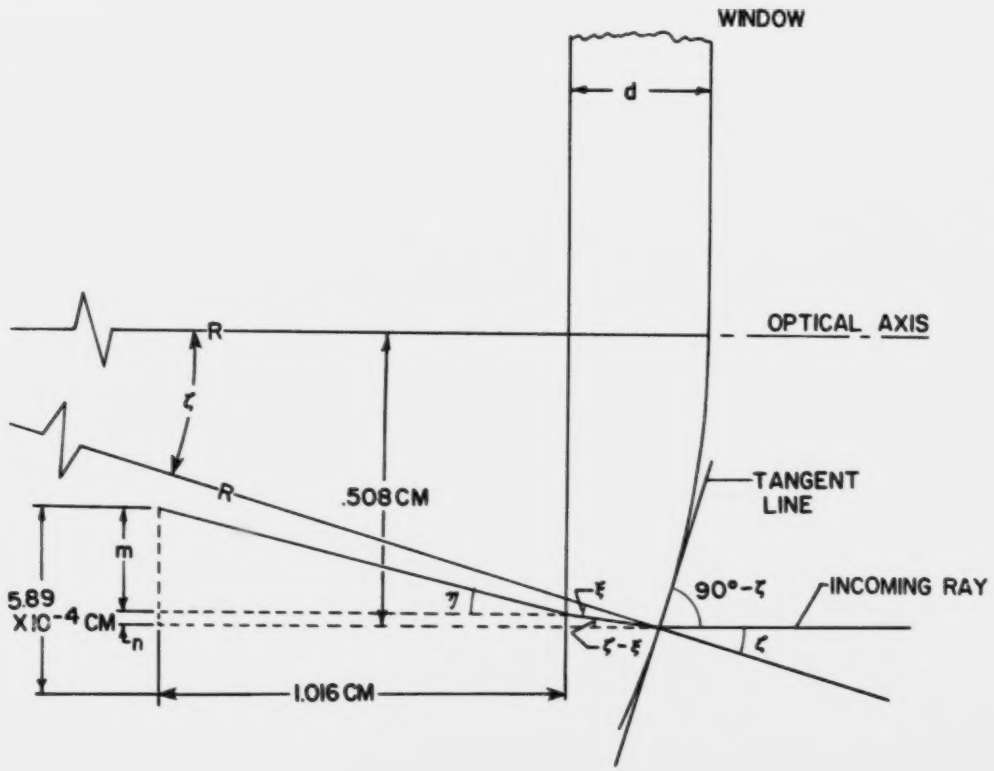

Figure 10.- Diagram for calculating error caused by window curvature.

one side of the window. Index of refraction of the glass is assumed to be 1.5. The angle ζ of the incoming ray can be described by

$$\sin \zeta = \frac{0.508}{R} \tag{1}$$

$$\tan \zeta = \frac{0.508}{\sqrt{R^2 - 0.2581}} \tag{2}$$

$$\cos \zeta = \frac{\sqrt{R^2 - 0.2581}}{R} \tag{3}$$

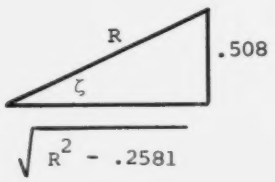

where R is the radius of curvature. According to the simple relation governing refraction, the angle ξ of the ray refracted by the curved window surface is

$$\frac{\sin \xi}{\sin \zeta} = \frac{1}{1.5} \tag{4}$$

$$\xi = \sin^{-1}\left(\frac{\sin \zeta}{1.5}\right) \tag{5}$$

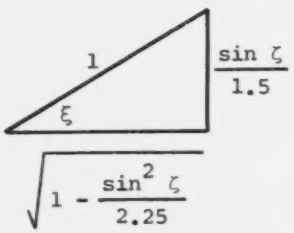

The displacement n (fig. 10) is then

$$n = d \tan \zeta - d \tan \xi = d\,(\tan \zeta - \tan \xi) = 0.635\,(\tan \zeta - \tan \xi) \tag{6}$$

Likewise, the angle η of the refracted ray exiting from the plane window surface is

$$\frac{\sin (\zeta - \xi)}{\sin \eta} = \frac{1}{1.5} \tag{7}$$

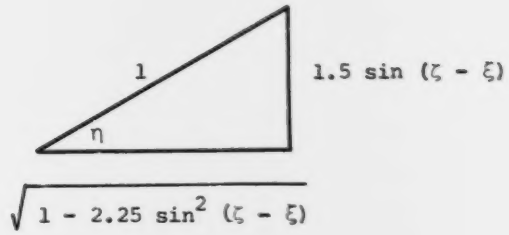

From equations (1) and (5)

$$\sin (\zeta - \xi) = \sin \left[\sin^{-1} \left(\frac{0.508}{R} \right) - \sin^{-1} \left(\frac{\sin \zeta}{1.5} \right) \right] \tag{8}$$

The displacement m (fig. 10) is

$$m = 1.016 \tan \eta \tag{9}$$

From equations (6) and (9), the total displacement is

$$m + n = 1.016 \tan \eta + 0.635 (\tan \zeta - \tan \xi) \tag{10}$$

For a 1-percent full-scale error,

$$5.891 \times 10^{-4} = 1.016 \left[\frac{1.5 \sin (\zeta - \xi)}{\sqrt{1 - 2.25 \sin^2 (\zeta - \xi)}} \right] + 0.635 (\tan \zeta - \tan \xi) \tag{11}$$

Substitution of equations (2), (5), and (8) in equation (11) gives

$$5.891 \times 10^{-4} = 1.016\left(\frac{1.5\left\{\sin\left[\sin^{-1}\left(\frac{0.508}{R}\right) - \sin^{-1}\left(\frac{\sin\zeta}{1.5}\right)\right]\right\}}{\sqrt{1 - 2.25\left\{\sin^2\left[\sin^{-1}\left(\frac{0.508}{R}\right) - \sin^{-1}\left(\frac{\sin\zeta}{1.5}\right)\right]\right\}}}\right)$$

$$+ 0.635\left(\frac{0.508}{\sqrt{R^2 - 0.258}} - \frac{\frac{\sin\zeta}{1.5}}{\sqrt{1 - \frac{\sin^2\zeta}{2.25}}}\right) \tag{12}$$

In equation (12), $\sin\zeta$ is required. From the following sketch, let

$$x^2 + y^2 = R^2 \tag{13}$$

$$\frac{dy}{dx} = \pm\frac{1}{2}\left(R^2 - x^2\right)^{-1/2}(-2x) \tag{14}$$

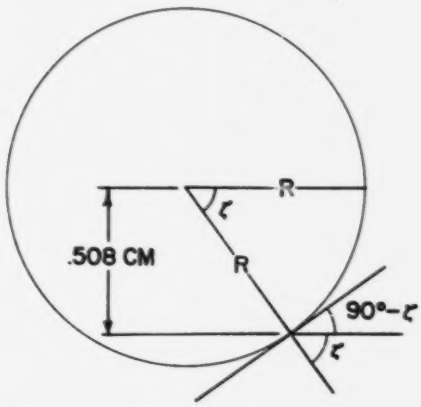

When $y = 0.508$ cm,

$$x = \pm\sqrt{R^2 - 0.258} \tag{15}$$

Substitute equation (15) in equation (14) to obtain

$$\frac{dy}{dx} = \pm\frac{1}{2}\left(R^2 - R^2 + 0.258\right)^{-1/2}\left(\pm 2\sqrt{R^2 - 0.258}\right)$$

$$= 1.969\sqrt{R^2 - 0.258} \tag{16}$$

Thus,

$$\tan\ (90^{o} - \zeta) = \frac{dy}{dx} = 1.969\sqrt{R^2 - 0.258} \tag{17}$$

$$\frac{\cos\ \zeta}{\sin\ \zeta} = 1.969\sqrt{R^2 - 0.258} \tag{18}$$

Substitute equation (3) in equation (18) to obtain

$$\sin\ \zeta = \frac{\sqrt{R^2 - 0.258}}{R(1.969)\sqrt{R^2 - 0.258}} = \frac{1}{1.969R} = \frac{0.5079}{R} \tag{19}$$

Finally, substitute equation (19) in equation (12) to obtain

$$5.891 \times 10^{-4} = 1.016\left(\frac{1.5\left\{\sin\left[\sin^{-1}\left(\frac{0.508}{R}\right) - \sin^{-1}\left(\frac{0.3386}{R}\right)\right]\right\}}{\sqrt{1 - 2.25\left\{\sin^2\left[\sin^{-1}\left(\frac{0.508}{R}\right) - \sin^{-1}\left(\frac{0.3386}{R}\right)\right]\right\}}}\right)$$

$$+ 0.635\left(\frac{0.508}{\sqrt{R^2 - 0.258}} - \frac{0.3386}{R\sqrt{1 - \frac{0.11465}{R^2}}}\right) \tag{20}$$

For very large values of R, greater than 250 cm, equation (20) becomes

$$5.891 \times 10^{-4} = 1.524\left\{\sin\left[\sin^{-1}\left(\frac{0.508}{R}\right) - \sin^{-1}\left(\frac{0.3386}{R}\right)\right]\right\} + \frac{0.1076}{R} \tag{21}$$

Solving equation (21) for R results in R = 619.8 cm. Thus, a radius of curvature of 619.8 cm corresponds to a 1-percent full-scale error. For a plano-convex lens

$$\frac{1}{F} = (n - 1)\left(\frac{1}{R_1} - \frac{1}{R_2}\right) \tag{22}$$

where n is the refractive index. For $1/R_2 = 0$ and $R_1 = 619.8$ cm, the focal length is $F = 1239.6$ cm = 0.081 diopter.

The curvature of all the windows used in the transducer was checked with an optical flat and red laser light with wavelength λ of approximately 700 nm (see sketch). The applicable equation is

$$Y = \pm\sqrt{2(S.H.)R - (S.H.)^2}$$

$$= \pm\sqrt{2\left(\frac{7.00 \times 10^{-5}}{2}\right)R - \left(\frac{7.00 \times 10^{-5}}{2}\right)^2} \tag{23}$$

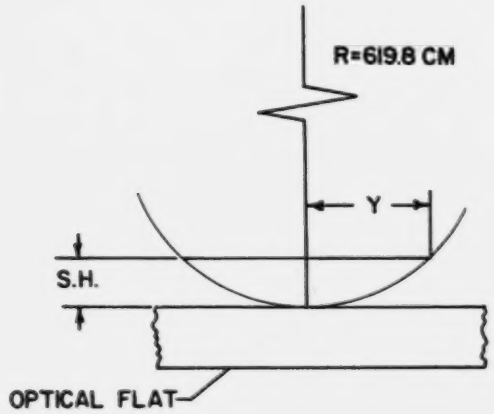

where Y is the distance to the first dark interference ring when the sagittal height (S.H.) is $\lambda/2$. The transducer windows were at least twice as flat as those that produced a 1-percent full-scale error. Thus, the radius of curvature of the transducer windows was greater than 1239.5 cm. Calculating error due to window curvature for this value of R (eq. (21)) results in a maximum full-scale displacement error of 2.946×10^{-4} cm or 0.5 percent.

When data reduction is performed as recommended, the nonlinearity of the photocell and electronic system output would give insignificant error. The error in the peak values of torsional displacement θ used in the computation would conservatively be less than ±0.5 percent. Thus, the total fractional standard deviation of the mean in measuring θ, the initial torsional amplitude, is

$$\frac{\sigma_{\theta_0}}{\theta_0} = \sqrt{(0.5 \text{ percent})^2 + (0.5 \text{ percent})^2} = 0.707 \text{ percent} \tag{24}$$

The basic equations used in data reduction are derived in appendix C, and the method of obtaining damping coefficient from measurements of three successive peak amplitudes is described in appendix D. The damping coefficient is defined by equation (C21) to be

$$c = \frac{a}{\sqrt{1 + a^2}} \tag{25}$$

where a is calculated according to equation (D15) as

$$a = \frac{\ln\left(\frac{\theta_0 - \theta_1}{\theta_1 - \theta_2}\right)}{2\pi} \tag{26}$$

where θ_0, θ_1, and θ_2 are three successive (all positive or all negative) peak amplitudes of the system response curve, as seen in figure 11.

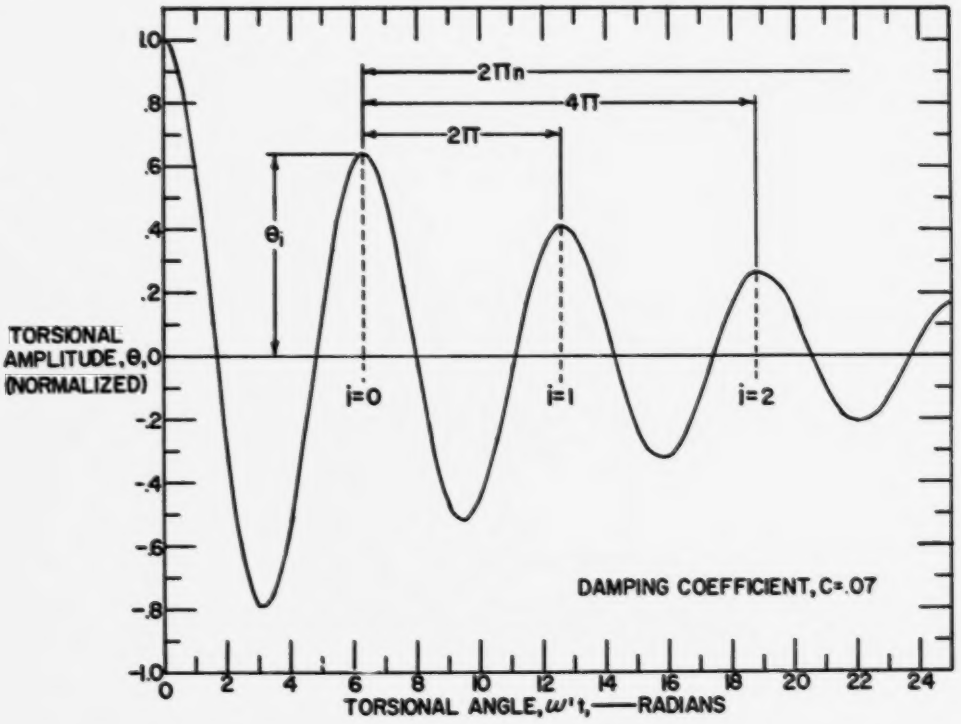

Figure 11.- Torsional amplitude versus time plot of a damped, second order, fully oscillating torsional system.

The damping error based on the measurement of three successive peak amplitudes is now computed as follows:

$$dc = \frac{-a^2\, da}{(1 + a^2)^{3/2}} + \frac{da}{(1 + a^2)^{1/2}} = \frac{da}{(1 + a^2)^{3/2}} \tag{27}$$

$$da = \frac{\partial a}{\partial \theta_0} d\theta_0 + \frac{\partial a}{\partial \theta_1} d\theta_1 + \frac{\partial a}{\partial \theta_2} d\theta_2$$

$$= \frac{1}{2\pi(\theta_0 - \theta_1)}\left[d\theta_0 - \left(\frac{\theta_0 - \theta_2}{\theta_1 - \theta_2}\right)d\theta_1 + \left(\frac{\theta_0 - \theta_1}{\theta_1 - \theta_2}\right)d\theta_2\right] \tag{28}$$

$$\sigma_a = \frac{1}{2\pi(\theta_0 - \theta_1)}\left[\sigma^2_{\theta_0} + \left(\frac{\theta_0 - \theta_2}{\theta_1 - \theta_2}\right)^2 \sigma^2_{\theta_1} + \left(\frac{\theta_0 - \theta_1}{\theta_1 - \theta_2}\right)^2 \sigma^2_{\theta_2}\right]^{1/2} \tag{29}$$

$$\frac{dc}{c} = \frac{da(1 + a^2)^{1/2}}{(1 + a^2)^{3/2} a} = \frac{da}{a(1 + a^2)} \tag{30}$$

$$\frac{dc}{c} = \frac{\frac{1}{2\pi(\theta_0 - \theta_1)}\left[d\theta_0 - \left(\frac{\theta_0 - \theta_2}{\theta_1 - \theta_2}\right)d\theta_1 + \left(\frac{\theta_0 - \theta_1}{\theta_1 - \theta_2}\right)d\theta_2\right]}{\frac{\ln\left(\frac{\theta_0 - \theta_1}{\theta_1 - \theta_2}\right)}{2\pi}\left\{1 + \left[\frac{\ln\left(\frac{\theta_0 - \theta_1}{\theta_1 - \theta_2}\right)}{2\pi}\right]^2\right\}} \tag{31}$$

In equation (31), it must be remembered that $d\theta_0$, $d\theta_1$, and $d\theta_2$ are independent errors even though their amplitudes are dependent on θ_0. If all the errors are of the same magnitude and sign, then the error dc/c is 0. This is not a very reliable estimate of the error. The maximum error would occur when $d\theta_1$ is opposite in sign to $d\theta_0$ and $d\theta_2$. The standard deviation of the mean, which is independent of sign, is always preferable for giving the precision and accuracy of the measurement and is used in the following calculation.

Let n_1 be the fractional "overshoot"; then

$$\frac{\sigma_c}{c} = \left(\frac{\left[\frac{\sigma_{\theta_0}}{2\pi\theta_0\left(1 - n_1^2\right)} \right]^2 \left[1 + \left(-\frac{1 - n_1^4}{n_1^2 - n_1^4} \right)^2 \left(n_1^2\right)^2 + \left(\frac{1 - n_1^2}{n_1^2 - n_1^4} \right)^2 \left(n_1^4\right)^2 \right]}{\left[\frac{\ln\left(\frac{1 - n_1^2}{n_1^2 - n_1^4} \right)}{2\pi} \right]^2 \left\{ 1 + \left[\frac{\ln\left(\frac{1 - n_1^2}{n_1^2 - n_1^4} \right)}{2\pi} \right]^2 \right\}^2} \right)^{1/2} \tag{32}$$

$$\frac{\sigma_c}{c} = \frac{\sigma_{\theta_0}}{\theta_0} \left\{ \frac{2^{1/2}\left(1 + n_1^2 + n_1^4\right)^{1/2}}{\left(1 - n_1^2\right)\left(\ln \frac{1}{n_1^2}\right)\left[1 + \left(\frac{\ln \frac{1}{n_1^2}}{2\pi} \right)^2 \right]} \right\} \tag{33}$$

A practical range of damping coefficients c, taken from reference 1, is 0.015 to 0.50. For $c = 0.50$, the overshoot of alternate peaks is approximately 16 percent, and for $c = 0.015$, the overshoot is 95.4 percent. Calculation of maximum error for $c = 0.50$ with $\sigma_{\theta_0}/\theta_0 = 0.707$ percent is

$$\frac{\sigma_c}{c} = \frac{\sigma_{\theta_0}}{\theta_0} \left\{ \frac{2^{1/2}(1 + 0.16^2 + 0.16^4)^{1/2}}{(1 - 0.16^2)\left(\ln \frac{1}{0.16^2}\right)\left[1 + \left(\frac{\ln \frac{1}{0.16^2}}{2\pi} \right)^2 \right]} \right\} = 0.212 \text{ percent} \tag{34}$$

and the maximum error for $c = 0.015$ is

$$\frac{\sigma_c}{c} = \frac{\sigma_{\theta_0}}{\theta_0} \left\{ \frac{2^{1/2}(1 + 0.954^2 + 0.954^4)^{1/2}}{(1 - 0.954^2)\left(\ln \frac{1}{0.954^2}\right)\left[1 + \left(\frac{\ln \frac{1}{0.954^2}}{2\pi} \right)^2 \right]} \right\} = 195 \text{ percent} \tag{35}$$

Although a 195-percent relative standard deviation may seem large, it does approach infinity as c approaches zero. At that point, σ_c/c becomes indeterminate. For the example given, $c = 0.015 \pm 1.95(0.015)$ results in 0.044 as the upper limit and -0.014 as the lower limit. Since negative damping does not exist, the lower limit is zero. Thus the bounds of the damping are from zero to 0.044 with a most probable value of 0.015. As damping increases, σ_c/c decreases. If three alternate peaks rather than three successive peaks were used, the reader can verify (from eq. (D16)) that σ_c/c would be greater than the three-successive-peak method by a factor of

$$\frac{2(n_1 + 1)}{\left(n_1^2 - n_1 + 1\right)^{1/2}} \tag{36}$$

This factor has a maximum value of 4.0 for $n_1 = 1.0$.

The rigidity or torsional spring constant K is given by equation (C14) as

$$K = \frac{4\pi^2 J}{T^2} + c^2\omega^2 J$$

$$= J\omega'^2\left[1 + \frac{c^2}{(1 - c^2)}\right] = J\omega'^2\left(\frac{1}{1 - c^2}\right) \tag{37}$$

where J is the torsional moment of inertia, T is the period of oscillation, and ω and ω' are the natural and damped angular velocities, and where (eqs. (C10) and (C13))

$$\omega' = (1 - c^2)^{1/2}\omega \qquad \text{and} \qquad \omega' T = 2\pi \tag{38}$$

The error dK can readily be obtained as was demonstrated previously for dc, by taking

$$dK = \frac{\partial K}{\partial J} dJ + \frac{\partial K}{\partial \omega'} d\omega' + \frac{\partial K}{\partial c} dc \tag{39}$$

or

$$\sigma_K = \left[\left(\frac{\partial K}{\partial J}\right)^2 \sigma_J^2 + \left(\frac{\partial K}{\partial \omega}\right)^2 \sigma_{\omega'}^2 + \left(\frac{\partial K}{\partial c}\right)^2 \sigma_c^2\right]^{1/2} \tag{40}$$

From equation (37),

$$\ln K = \ln J + 2 \ln \omega' - \ln (1 - c^2) \tag{41}$$

For the relative error,

$$\frac{dK}{K} = \frac{dJ}{J} + 2 \frac{d\omega'}{\omega'} + \frac{2c^2}{1 - c^2} \frac{dc}{c} \tag{42}$$

or

$$\frac{\sigma_K}{K} = \left[\left(\frac{\sigma_J}{J} \right)^2 + 4 \left(\frac{\sigma_{\omega'}}{\omega'} \right)^2 + 4 \left(\frac{c^2}{1 - c^2} \right)^2 \left(\frac{\sigma_c}{c} \right)^2 \right]^{1/2} \tag{43}$$

Torsional amplitude can be given by

$$\theta = \frac{T_o L}{G J_A} \tag{44}$$

where T_o is the torque in the torsional member of length L, G is shear modulus, and J_A is the polar areal moment of inertia of the torsional member. Then, since $T_o/\theta = K$,

$$G = \frac{T_o L}{\theta J_A} = \frac{KL}{J_A} = \frac{J\omega'^2 \left(\frac{1}{1 - c^2} \right)}{J_A} L \tag{45}$$

For the relative error in shear modulus,

$$\ln G = \ln J + 2 \ln \omega' - \ln (1 - c^2) + \ln L - \ln J_A \tag{46}$$

$$\frac{dG}{G} = \frac{dJ}{J} + 2 \frac{d\omega'}{\omega'} + \frac{2c^2}{1 - c^2} \frac{dc}{c} + \frac{dL}{L} - \frac{dJ_A}{J_A} \tag{47}$$

or

$$\frac{\sigma_G}{G} = \left[\left(\frac{\sigma_J}{J} \right)^2 + 4 \left(\frac{\sigma_{\omega'}}{\omega'} \right)^2 + 4 \left(\frac{c^2}{1 - c^2} \right)^2 \left(\frac{\sigma_c}{c} \right)^2 + \left(\frac{\sigma_L}{L} \right)^2 + \left(- \frac{\sigma_{J_A}}{J_A} \right)^2 \right]^{1/2} \tag{48}$$

DISCUSSION

The optical system utilizes a newly invented technique for which a patent has been obtained (ref. 6). This consists of the refracting quartz windows used in conjunction with the differential photocell for producing a null signal. The error contributions from these components can be controlled to insignificance, with no undue demands made for their fabrication. This factor together with the null signal method of obtaining output, which is probably the most advantageous in transducer design, contributes to producing an optimal transducer package. An analysis of the electronic circuit did not predict quirks that developed during laboratory testing, and numerous additional tests were made to optimize the design.

One of the quirks that appeared, which could not be eliminated by design, was a modulation which occurred on the decay curve envelope. A basic analysis isolated the cause to any system with torsion in it that had nonstraight-line coincidence of the torsional and physical axes of its torsion member. This produces a time variation of the torque in the torsion member and a time varying coefficient of the angular displacement in the differential equation of motion for the system. This time variation causes the modulation of the envelope. In a flexible suspension, one of the most likely causes for misalignment of the torsional and physical axes is rigid end point fastenings. These are the most commonly used in practice, and they cause axial misalignment of the suspension when it is nontorsionally perturbed. Relatively unrelated transducer systems such as those using vibrating wires with clamped ends for measuring angular rate have produced odd outputs which can be explained by this analysis, since some torsion inadvertently is built into the fixed end point fastenings. To minimize or prevent the effects of axial misalignment, care should be taken to ensure that the torsional member axis is straight. If end pinning devices are attached to it, these should be made colinear with the axis. The end fastenings may also be made rigid to torsion but soft to plane motion. Finally, unless a perfect end fastening is used (which is unlikely), some form of stabilizer should be used to prevent perturbations from bending the torsional axis.

The detailed error analysis which was performed was for the purpose of producing a precise and accurate transducer. However, the results of this effort can also be used for selecting the method or methods which give least error in the data reduction and for explaining why more scatter occurs over one range of the data than over another. Also, until now, it has been believed that obtaining G, the shear modulus, of the composite structure of the polymer-impregnated braid used for the torsional suspension was not feasible. In equation (48), which gives the relative error of G, all factors contributing to the relative error can readily be determined with the exception of dJ_A/J_A, where J_A is the polar areal moment of inertia. Cross sections of the polymer-impregnated braid can be obtained by methods similar to those used in getting tissue or metallurgical specimens. From these, it is assumed, on a statistical basis, that a most probable areal configuration may be obtained. It would then be a simple matter to obtain the areal moment of inertia of the composite constituents, the relative error of G, and G itself of the composite braid. By superposition, the G value of the polymer only could then be determined.

Another factor of interest is the initiation of the free torsional oscillations of the pendulum. In order to guarantee repeatability of results and avoid introducing a forcing function into the initial conditions of the pendulum release, the initial starting amplitude, as measured from the average pendulum position, should be kept constant and held sufficiently long that its constancy is beyond doubt. Release should then be sharp and should introduce no perturbations. The release mechanism in this transducer meets all these criteria.

CONCLUDING REMARKS

An improved torsional braid pendulum transducer has been designed which is considered an advance in the state of the art. The transducer has been described and its precision and accuracy have been analyzed. This research has resulted in the following findings:

1. Any torsional system, or system with torsion in it, having misalignment of the torsional and physical axes of its torsion member experiences a time variation of its torque output when the system is in the dynamic state. This results in a time varying torque in the torsion member and a time variable coefficient for torsional amplitude in the differential equation of motion for the system. The result is a modulation of the normal output of a freely oscillating, torsional system. To minimize these effects in flexible torsion members, which are normally undesirable, care should be taken to ensure that the torsional member axis and its end pinning devices are colinear. A suspension system that is rigid to torsional motion but soft to plane motion may be used. Some form of stabilizer to prevent perturbations from bending the torsion member axis should be used.

2. The step input for exciting the torsion pendulum gave a smooth, crisp release from the same starting amplitude.

3. The null method employed in this transducer for obtaining the output makes it virtually insensitive to any but torsional motions.

4. The maximum relative error (due to window curvature) in the torsional amplitudes for this system is 0.7 percent. This results in relative errors in the measurement of the damping ratio c of 195 percent for $c = 0.015$ and 0.212 percent for $c = 0.50$; this error decreases as the damping ratio increases. Since rigidity and shear modulus are dependent on c, more scatter in the data should be expected at the lower values of c for all three parameters.

5. To minimize error in data reduction, it is recommended that three successive (all positive or all negative) peaks be read out.

6. Making the windows optically flat to one-quarter of the wavelength of sodium light would make them a negligible source of error. The main source of error would then be the readout of the successive peak amplitudes, and any means to improve their accuracy would directly enhance the accuracy and precision of the quantities sought.

Langley Research Center
National Aeronautics and Space Administration
Hampton, VA 23665
February 25, 1981

APPENDIX A

COIL DESIGN

The design of the torsional braid pendulum displacement transducer included coils which cause the field that produces the initial torsional offset. The main consideration in designing the coils was to limit the current they draw from the power supply to a reasonable value. The formula for designing the coils is derived in this appendix.

A coil is desired with a given resistance and the dimensions shown in the following sketch:

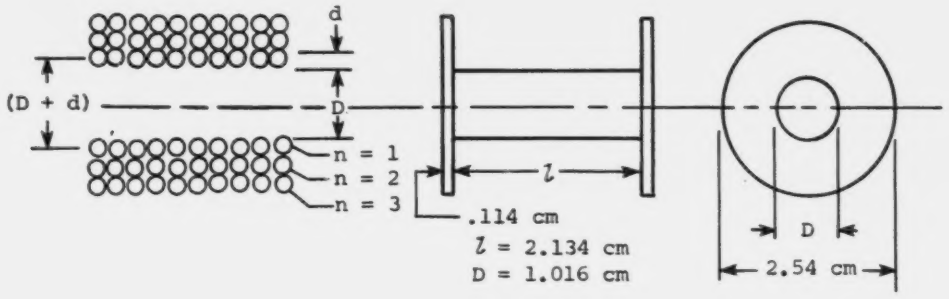

For the first layer of wire,

$$\pi(D + d)\,\frac{l}{d} = \text{Length of wire in layer 1} \tag{A1}$$

For the second layer,

$$\pi(D + 3d)\,\frac{l}{d} = \text{Length of wire in layer 2} \tag{A2}$$

For the nth layer,

$$\pi\left[D + (2n - 1)d\right]\frac{l}{d} = \text{Length of wire in layer } n \quad (n = 1,2,3,\ldots) \tag{A3}$$

From equation (A3), an arithmetic progression is obtained whose sum is

$$S = \frac{N}{2}\left\{\pi(D + d)\,\frac{l}{d} + \pi\left[D + (2N - 1)d\right]\frac{l}{d}\right\} \tag{A4}$$

$$= \frac{N\pi l}{2d}(2D + 2Nd) = \frac{N\pi l}{d}(D + Nd) \tag{A5}$$

where N is the number of layers in the coil. This sum is the total length of wire of diameter d in the coil. For the coil dimensions in the sketch,

$$S = \frac{N\pi(2.134)}{d}(1.016 + Nd) = 6.811\frac{N}{d} + 6.704N^2 \qquad (A6)$$

The diameter of the coil is also limited to 2.54 cm, that is,

$$2.54 \geq 2Nd + D$$

$$2.54 \geq 2Nd + 1.1016 \qquad (A7)$$

A coil with resistance of about 55 Ω is desired. Try wire with d = 0.0254 cm, which has a resistance of 110 Ω per 32 004 cm or 55 Ω per 16 002 cm. From equation (A6)

$$S = \frac{6.811}{0.0254}N + 6.704N^2 = 16\ 002 \qquad (A8)$$

$$6.704N^2 + 268.2N - 16\ 002 = 0 \qquad (A9)$$

Equation (A9) can be solved for N, which to a whole number is 33 layers. However,

$$2Nd + 1.1016 = 2(33)(0.0254) + 1.106 = 2.69$$

which violates equation (A7). Therefore 0.0254-cm-diameter wire is too large.

Try 32-gage wire with a 0.02032-cm diameter and resistance of 167.3 Ω per 30 480 cm. To provide coil resistance of 55 Ω, 22 layers were required. This resulted in a coil diameter of 1.91 cm, which was acceptable. The total number of turns is calculated as follows:

$$\frac{l}{d} = \frac{2.134}{0.02032} = 105 \text{ turns/layer}$$

$$105 \times 22 = 2310 \text{ turns}$$

APPENDIX B

PERTURBATION CALCULATIONS FOR THE TORSION PENDULUM

This discussion deals with the factors that affect the normal, regular decay curve of the damped oscillation of a compound torsion pendulum and the output of any system which is put in torsion and whose torsional axis becomes bent or deflected. A simple pendulum is first examined, and the final development is for the actual compound pendulum that is used in the transducer design. Consider a simple pendulum in torsion as is shown in sketch (a). If the axis of

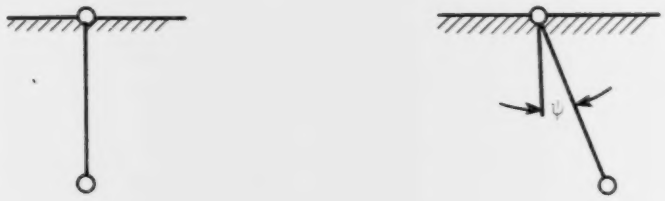

Sketch (a)

this pendulum is always a radial extension from the pin point, any torsional motion given to the pendulum would not be changed by any perturbation that displaced it from its statically stable position. This sort of suspension can be approached by using a very flexible diaphragm as the pin point for the pendulum suspension. This diaphragm is rigid to axial torsion and soft to moments at right angles to this torsion. Further, no linear forces acting on the center of mass can produce or change the torsion. The more usual situation is that the pin point is rigid and a perturbation producing a deflection of the axis changes the distribution of the torque from what it was previously. This results in modulations and other effects on the oscillation of the torsional pendulum (fig. 12). To illustrate the point, one mode of torque distribution is developed

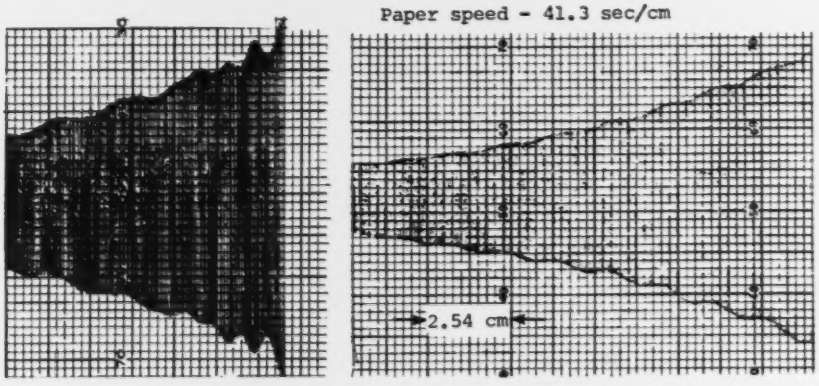

Figure 12.- Decay curve envelope modulation due to perturbations to a torsional pendulum.

sufficiently to show that the output is modulated. A second, more general torque distribution mode analysis is outlined, but the detailed solution is not made in this paper.

Depending on the torsional spring constant and the pendulum inertia, the torque can distribute itself as shown in sketch (b). The parallel component $T_{||}$ is $T_Y \cos \psi$ and the normal component T_N is $T_Y \sin \psi$. For small angles, the parallel component is much larger than the normal component, and although this development is for the parallel component only, the normal component of torque also contributes to the perturbation of the output, since it causes rotation of the pendulum. The torsional spring constant is $K = GJ_A/L$, and may be assumed constant because the effective length L under deflection remains essentially constant as does G, the shear modulus, and J_A, the areal moment of inertia. The bending stresses and strains, however, do have an effect on these parameters and cause coupling or interactions which are not well understood and were ignored in these calculations.

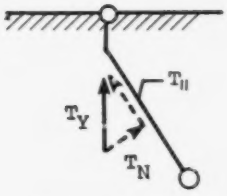

Sketch (b)

Assume that the pendulum is in torsion and receives a perturbation which moves it off axis to an angle ψ. Since the pendulum oscillates because of this, ψ is a function of time. The parallel component of torsion $T_{||}$ is dependent on ψ, and since this is the torsional spring torque in the differential equation of motion of the system, it changes the torsional amplitude θ from that obtained with the pendulum in axial alignment. This change, of course, is an error which should be eliminated. The normal component T_N moves the pendulum mass normally to the plane of the paper or in a conical motion. The change of ψ with time prevents a conical path but not the normal rotation. This motion also affects the output to produce an error which can be eliminated in the same way as the error due to the parallel component is eliminated.

For free oscillation, the differential equation now controlling θ in the offset axis, considering the parallel torque component only, is

$$J\ddot{\theta} + \ell\dot{\theta} + T_{||} = 0 \qquad \text{(B1)}$$

The design of the transducer called for a suspension which results in a compound pendulum. The following development for obtaining θ with perturbation for this situation is general until the algebra becomes too cumbersome and then actual values, taken from the designed pendulum, are used. Assume that a torsion T_Y has been induced at point B in sketch (c) and a perturbation produces ψ and ϕ. Then, $T_{||}$ which produces the torsional oscillation is $T_Y \cos \psi \cos (\phi - \psi)$.

APPENDIX B

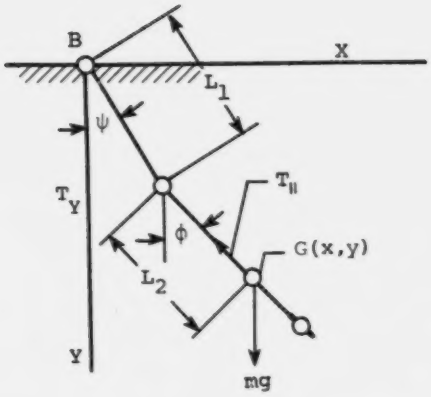

Sketch (c)

The conservative Lagrangian is now set up. The only effect of the damping force is to reduce ψ and ϕ more quickly; it does not alter the argument that modulation occurs. Thus, it is omitted in the following determination of ψ and ϕ. The position of the center of gravity (point G) in terms of the coordinate system shown in sketch (c) is

$$x = L_1 \sin \psi + L_2 \sin \phi \tag{B2}$$

$$y = L_1 \cos \psi + L_2 \cos \phi \tag{B3}$$

The velocity components of the center of gravity at point G are

$$\dot{x} = L_1(\cos \psi)\dot{\psi} + L_2(\cos \phi)\dot{\phi} \tag{B4}$$

$$\dot{y} = -\left[L_1(\sin \psi)\dot{\psi} + L_2(\sin \phi)\dot{\phi}\right] \tag{B5}$$

so that the velocity v_G of point G is

$$v_G^2 = \left[L_1(\cos \psi)\dot{\psi} + L_2(\cos \phi)\dot{\phi}\right]^2 + \left[-L_1(\sin \psi)\dot{\psi} - L_2(\sin \phi)\dot{\phi}\right]^2 \tag{B6}$$

The kinetic energy of the pendulum is

$$T = \frac{1}{2} m v_G^2 + \frac{1}{2} I_G \dot{\phi}^2$$

where m is the pendulum mass and I_G is the mass moment of inertia about an axis through the center of gravity and perpendicular to the rod. Substituting equation (B6) results in

$$T = \frac{m}{2}\left\{\left[L_1(\cos\psi)\dot{\psi} + L_2(\cos\phi)\dot{\phi}\right]^2 + \left[L_1(\sin\psi)\dot{\psi} + L_2(\sin\phi)\dot{\phi}\right]^2\right\} + \frac{I_G\dot{\phi}^2}{2}$$

$$= \frac{m}{2}\left\{L_1^2\dot{\psi}^2 + L_2^2\dot{\phi}^2 + 2L_1L_2\left[\cos(\phi - \psi)\right]\dot{\psi}\dot{\phi}\right\} + \frac{I_G\dot{\phi}^2}{2} \qquad \text{(B7)}$$

To keep I_G general in terms of m and L_2, let

$$nmL_2^2 = I_G$$

where $L_2 = 25.96$ cm, $I_G = 4935$ g-cm^2, and $m = 38.7$ g. Then,

$$n = \frac{4935}{38.7(25.96)^2} = 0.189$$

Substituting $I_G = 0.189mL_2^2$ in equation (B7) gives

$$T = \frac{m}{2}\left\{L_1^2\dot{\psi}^2 + 1.19L_2^2\dot{\phi}^2 + 2L_1L_2\left[\cos(\phi - \psi)\right]\dot{\psi}\dot{\phi}\right\} \qquad \text{(B8)}$$

The potential energy of the system relative to its equilibrium position is

$$V = mg\left[(L_1 + L_2) - y\right] = mg\left[L_1(1 - \cos\psi) + L_2(1 - \cos\phi)\right] \qquad \text{(B9)}$$

where g is the acceleration due to gravity. By considering oscillations caused by small displacements, cubed and higher order terms are eliminated, and since

$$\cos(\phi - \psi) = 1 - \frac{(\phi^2 - 2\phi\psi + \psi^2)}{2} + \ldots$$

equations (B8) and (B9) become

$$T = \frac{m}{2}\left(L_1^2\dot{\psi}^2 + 1.19L_2^2\dot{\phi}^2 + 2L_1L_2\dot{\psi}\dot{\phi}\right) \qquad \text{(B10)}$$

$$V = \frac{mg}{2}\left(L_1\psi^2 + L_2\phi^2\right) \tag{B11}$$

Consider the Lagrangian, $\mathcal{L} = T - V$, with generalized coordinates ψ and ϕ represented by q_r:

$$\frac{d}{dt}\frac{\partial \mathcal{L}}{\partial \dot{q}_r} - \frac{\partial \mathcal{L}}{\partial q_r} = 0 \tag{B12}$$

which may be written as

$$\frac{d\left(\frac{\partial T}{\partial \dot{q}_r}\right)}{dt} + \frac{\partial V}{\partial q_r} = 0 \tag{B13}$$

since $-\partial V/\partial \dot{q}_r = 0$ and $\partial T/\partial q_r = 0$. Differentiate equations (B10) and (B11) to obtain

$$\frac{\partial T}{\partial \dot{\psi}} = \frac{m}{2}\left(2L_1{}^2\dot{\psi} + 2L_1L_2\dot{\phi}\right) = m\left(L_1{}^2\dot{\psi} + L_1L_2\dot{\phi}\right) \tag{B14}$$

$$\frac{\partial T}{\partial \dot{\phi}} = \frac{m}{2}\left[1.19(2)L_2{}^2\dot{\phi} + 2L_1L_2\dot{\psi}\right] = m\left(1.19L_2{}^2\dot{\phi} + L_1L_2\dot{\psi}\right) \tag{B15}$$

$$\frac{\partial V}{\partial \psi} = \frac{mg}{2}(2L_1\psi) = mgL_1\psi \tag{B16}$$

$$\frac{\partial V}{\partial \phi} = \frac{mg}{2}(2L_2\phi) = mgL_2\phi \tag{B17}$$

Equations (B14) to (B17) substituted in equation (B13) give the equations of motion:

$$\frac{d}{dt}\left[m\left(L_1{}^2\dot{\psi} + L_1L_2\dot{\phi}\right)\right] + mgL_1\psi = 0 \tag{B18}$$

$$\frac{d}{dt}\left[m\left(1.19L_2{}^2\dot{\phi} + L_1L_2\dot{\psi}\right)\right] + mgL_2\phi = 0 \tag{B19}$$

APPENDIX B

From equation (B18),

$$L_1\ddot{\psi} + L_2\ddot{\phi} + g\psi = 0 \tag{B20}$$

From equation (B19),

$$L_1\ddot{\psi} + 1.19L_2\ddot{\phi} + g\phi = 0 \tag{B21}$$

Equations (B20) and (B21) give

$$\begin{vmatrix} L_1p^2 - g & L_2p^2 \\ L_1p^2 & 1.19L_2p^2 - g \end{vmatrix} = 0 \tag{B22}$$

where the p's are the angular frequencies of the principal modes of oscillation. Thus, from equation (B22),

$$0.19L_1L_2p^4 - (L_1 + 1.19L_2)gp^2 + g^2 = 0$$

where p^2 is

$$p_{1,2}^2 = \frac{(L_1 + 1.19L_2)g \pm \sqrt{(L_1 + 1.19L_2)^2g^2 - 4(0.19)L_1L_2g^2}}{2(0.19L_1L_2)}$$

$$= \frac{(L_1 + 1.19L_2)g \pm \sqrt{L_1^2g^2 + 1.62L_1L_2g^2 + (1.19L_2)^2g^2}}{0.38L_1L_2} \tag{B23}$$

From equation (B23), it can be seen that both roots are positive. The periods are then

$$T_1 = \frac{2\pi}{p_1} \tag{B24}$$

$$T_2 = \frac{2\pi}{p_2} \tag{B25}$$

where p_1 and p_2 are the positive roots of p_1^2 and p_2^2. The angles ψ and ϕ are still needed. Therefore, subtract equation (B20) from equation (B21) to get

$$0.19L_2\ddot{\phi} + g(\phi - \psi) = 0$$

$$\ddot{\phi} + 5.26\,\frac{g}{L_2}\,\phi - \frac{5.26g\psi}{L_2} = 0 \tag{B26}$$

Multiply equation (B20) by 1.19 and subtract equation (B21) to get

$$\ddot{\psi} + 6.26\,\frac{g\psi}{L_1} - 5.26\,\frac{g}{L_1}\,\phi = 0 \tag{B27}$$

In operator form, equations (B26) and (B27) are

$$\left(D^2 + 5.26\,\frac{g}{L_2}\right)\phi - 5.26\,\frac{g}{L_2}\,\psi = 0 \tag{B28}$$

$$-5.26\,\frac{g}{L_1}\,\phi + \left(D^2 + 6.26\,\frac{g}{L_1}\right)\psi = 0 \tag{B29}$$

The determinant of equations (B28) and (B29) is

$$\Delta = \begin{vmatrix} D^2 + 5.26\,\dfrac{g}{L_2} & -5.26\,\dfrac{g}{L_2} \\ -5.26\,\dfrac{g}{L_1} & D^2 + 6.26\,\dfrac{g}{L_1} \end{vmatrix}$$

Let $5.26\,\dfrac{g}{L_2} = M$; then

$$\Delta = D^4 + \left(6.26\,\frac{g}{L_1} + M\right)D^2 + M\left(6.26\,\frac{g}{L_1}\right) - M\left(5.26\,\frac{g}{L_1}\right)$$

$$= D^4 + \left(6.26\,\frac{g}{L_1} + M\right)D^2 + M\,\frac{g}{L_1} \tag{B30}$$

Let $N = 6.26\,\dfrac{g}{L_1} + M$; then

$$\Delta = D^4 + ND^2 + \frac{Mg}{L_1} \tag{B31}$$

APPENDIX B

$$\left(D^4 + ND^2 + \frac{Mg}{L_1}\right)\phi = \begin{vmatrix} 0 & -M \\ 0 & \left(D^2 + 6.26\,\frac{g}{L_1}\right) \end{vmatrix}$$

$$\left(D^4 + ND^2 + \frac{Mg}{L_1}\right)\phi = 0 \tag{B32}$$

$$\left(D^4 + ND^2 + \frac{Mg}{L_1}\right)\psi = \begin{vmatrix} D^2 + M & 0 \\ -5.26\,\frac{g}{L_1} & 0 \end{vmatrix} = 0$$

$$\left(D^4 + ND^2 + \frac{Mg}{L_1}\right)\psi = 0 \tag{B33}$$

For both ϕ and ψ,

$$r^4 + Nr^2 + \frac{Mg}{L_1} = 0$$

where r is a characteristic root. Then

$$r^2 = \frac{-N \pm \sqrt{N^2 - 4\,\frac{Mg}{L_1}}}{2} = \frac{\left(-M - 6.26\,\frac{g}{L_1}\right) \pm \sqrt{\left(6.26\,\frac{g}{L_1} + M\right)^2 - 4\,\frac{Mg}{L_1}}}{2}$$

$$r^2 = \frac{g\left[\left(-\frac{5.26}{L_2} - \frac{6.26}{L_1}\right) \pm \sqrt{\frac{39.2}{{L_1}^2} + \frac{44.8}{L_1 L_2} + \frac{27.7}{{L_2}^2}}\right]}{2} \tag{B34}$$

At this point the following actual pendulum values are substituted into equation (B34):

$L_1 = 21.84$ cm

$L_2 = 25.96$ cm

APPENDIX B

$$r^2 = 980\,\frac{\left(-\frac{5.26}{25.96} - \frac{6.26}{21.84}\right) \pm \sqrt{\frac{39.2}{(21.84)^2} + \frac{44.8}{(21.84)(25.96)} + \frac{27.7}{(25.96)^2}}}{2}$$

$$= 980\left(\frac{-0.489 \pm 0.202}{2}\right) \tag{B35}$$

$$r_1^2 = -338.6$$

$$r_2^2 = -140.6$$

$$r_1 = \pm 18.4i \tag{B36}$$

$$r_2 = \pm 11.9i \tag{B37}$$

Equations (B36) and (B37) give the solution to the differential equations. Since there is no particular solution, let

$$\psi = c_1 e^{(18.4i)t} + c_2 e^{(-18.4i)t} + c_3 e^{(11.9i)t} + c_4 e^{(-11.9i)t} \tag{B38}$$

$$\phi = d_1 e^{(18.4i)t} + d_2 e^{(-18.4i)t} + d_3 e^{(11.9i)t} + d_4 e^{(-11.9i)t} \tag{B39}$$

Differentiate equations (B38) and (B39) to obtain

$$\dot{\psi} = c_1 e^{(18.4i)t}(18.4i) + c_2 e^{(-18.4i)t}(-18.4i) + c_3 e^{(11.9i)t}(11.9i) + c_4 e^{(-11.9i)t}(-11.9i) \tag{B40}$$

$$\ddot{\psi} = c_1 e^{(18.4i)t}(-1)(18.4)^2 + c_2 e^{(-18.4i)t}(-1)(18.4)^2 + c_3 e^{(11.9i)t}(-1)(11.9)^2 + c_4 e^{(-11.9i)t}(-1)(11.9)^2 \tag{B41}$$

$$\dot{\phi} = d_1 e^{(18.4i)t}(18.4i) + d_2 e^{(-18.4i)t}(-18.4i) + d_3 e^{(11.9i)t}(11.9i) + d_4 e^{(-11.9i)t}(-11.9i) \tag{B42}$$

$$\ddot{\phi} = d_1 e^{(18.4i)t}(-1)(18.4)^2 + d_2 e^{(-18.4i)t}(-1)(18.4)^2$$
$$+ d_3 e^{(11.9i)t}(-1)(11.9)^2 + d_4 e^{(-11.9i)t}(-1)(11.9)^2 \quad \text{(B43)}$$

Substituting equations (B38), (B39), and (B43) in equation (B26) gives

$$-d_1 e^{(18.4i)t}(18.4)^2 - d_2 e^{(-18.4i)t}(18.4)^2 - d_3 e^{(11.9i)t}(11.9)^2$$
$$- d_4 e^{(-11.9i)t}(11.9)^2 + 5.26 \frac{g}{L_2}\left[d_1 e^{(18.4i)t} + d_2 e^{(-18.4i)t} + d_3 e^{(11.9i)t}\right.$$
$$\left. + d_4 e^{(-11.9i)t} - c_1 e^{(18.4i)t} - c_2 e^{(-18.4i)t} - c_3 e^{(11.9i)t} - c_4 e^{(-11.9i)t}\right] = 0 \quad \text{(B44)}$$

Substituting equations (B38), (B39), and (B41) in equation (B27) gives

$$-c_1 e^{(18.4i)t}(18.4)^2 - c_2 e^{(-18.4i)t}(18.4)^2 - c_3 e^{(11.9i)t}(11.9)^2$$
$$- c_4 e^{(-11.9i)t}(11.9)^2 + 6.26 \frac{g}{L_1}\left[c_1 e^{(18.4i)t} + c_2 e^{(-18.4i)t}\right.$$
$$\left. + c_3 e^{(11.9i)t} + c_4 e^{(-11.9i)t}\right] - 5.26 \frac{g}{L_1}\left[d_1 e^{(18.4i)t}\right.$$
$$\left. + d_2 e^{(-18.4i)t} + d_3 e^{(11.9i)t} + d_4 e^{(-11.9i)t}\right] = 0 \quad \text{(B45)}$$

Equating equations (B44) and (B45) gives

$$-d_1 e^{(18.4i)t}(18.4)^2 - d_2 e^{(-18.4i)t}(18.4)^2 - d_3 e^{(11.9i)t}(11.9)^2$$
$$- d_4 e^{(-11.9i)t}(11.9)^2 + 5.26 \frac{g}{L_2}\left[d_1 e^{(18.4i)t} + d_2 e^{(-18.4i)t} + d_3 e^{(11.9i)t}\right.$$
$$\left. + d_4 e^{(-11.9i)t} - c_1 e^{(18.4i)t} - c_2 e^{(-18.4i)t} - c_3 e^{(11.9i)t} - c_4 e^{(-11.9i)t}\right]$$
$$= -c_1 e^{(18.4i)t}(18.4)^2 - c_2 e^{(-18.4i)t}(18.4)^2 - c_3 e^{(11.9i)t}(11.9)^2$$
$$- c_4 e^{(-11.9i)t}(11.9)^2 + 6.26 \frac{g}{L_1}\left[c_1 e^{(18.4i)t} + c_2 e^{(-18.4i)t}\right.$$
$$\left. + c_3 e^{(11.9i)t} + c_4 e^{(-11.9i)t}\right] - 5.26 \frac{g}{L_1}\left[d_1 e^{(18.4i)t}\right.$$
$$\left. + d_2 e^{(-18.4i)t} + d_3 e^{(11.9i)t} + d_4 e^{(-11.9i)t}\right] \quad \text{(B46)}$$

From equation (B46),

$$\left[-(18.4)^2 d_1 + 5.26 \frac{g}{L_2} d_1 - 5.26 \frac{g}{L_2} c_1 + (18.4)^2 c_1 - 6.26 \frac{g}{L_1} c_1 + 5.26 \frac{g}{L_1} d_1\right] e^{(18.4i)t} = 0$$

$$-338.6d_1 + 198.6d_1 + 236.0d_1 - 198.6c_1 + 338.6c_1 - 280.9c_1 = 0$$

$$d_1 = \frac{140.9c_1}{96} = 1.47c_1 \qquad \text{(B47)}$$

From equation (B46),

$$\left[-(18.4)^2 d_2 + 5.26 \frac{g}{L_2} d_2 - 5.26 \frac{g}{L_2} c_2 + (18.4)^2 c_2 - 6.26 \frac{g}{L_1} c_2 + 5.26 \frac{g}{L_1} d_2\right] e^{(-18.4i)t} = 0$$

$$-338.6d_2 + 198.6d_2 + 236.0d_2 - 198.6c_2 + 338.6c_2 - 280.9c_2 = 0$$

$$d_2 = 1.47c_2 \qquad \text{(B48)}$$

From equation (B46),

$$\left[-(11.9)^2 d_3 + 5.26 \frac{g}{L_2} d_3 - 5.26 \frac{g}{L_2} c_3 + (11.9)^2 c_3 - 6.26 \frac{g}{L_1} c_3 + 5.26 \frac{g}{L_1} d_3\right] e^{(11.9i)t} = 0$$

$$-141.6d_3 + 198.6d_3 + 236.0d_3 - 198.6c_3 + 141.6c_3 - 280.9c_3 = 0$$

$$d_3 = 1.15c_3 \qquad \text{(B49)}$$

APPENDIX B

From equation (B46),

$$\left[-(11.9)^2 d_4 + 5.26 \frac{g}{L_2} d_4 - 5.26 \frac{g}{L_2} c_4 + (11.9)^2 c_4 - 6.26 \frac{g}{L_1} c_4 + 5.26 \frac{g}{L_1} d_4\right] e^{(-11.9i)t} = 0$$

$$-141.6d_4 + 198.6d_4 + 236.0d_4 - 198.6c_4 + 141.6c_4 - 280.9c_4 = 0$$

$$d_4 = 1.15c_4 \tag{B50}$$

From equations (B47) to (B50), only four arbitrary constants remain; these inserted in equation (B39) give

$$\phi = 1.47c_1 e^{(18.4i)t} + 1.47c_2 e^{(-18.4i)t} + 1.15c_3 e^{(11.9i)t} + 1.15c_4 e^{(-11.9i)t} \tag{B51}$$

The c's are now evaluated.

At t = 0, an initial offset is assumed as shown in sketch (d):

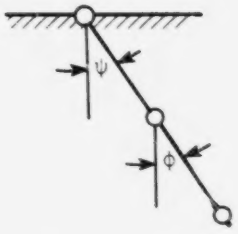

Sketch (d)

$$\psi_o = \phi_o \tag{B52}$$

(Note that the most general initial condition should be $\psi_o \neq \phi_o$ which would make the derivation unwieldy. The assumed condition frequently occurs.) Substituting these values into equations (B38) and (B51) results in

$$\psi_o = c_1 + c_2 + c_3 + c_4 \tag{B53}$$

$$\phi_o = 1.47c_1 + 1.47c_2 + 1.15c_3 + 1.15c_4 = \psi_o \tag{B54}$$

APPENDIX B

Differentiating equations (B38) and (B51) results in

$$\dot{\psi} = (18.4i)c_1e^{(18.4i)t} - (18.4i)c_2e^{(-18.4i)t} + (11.9i)c_3e^{(11.9i)t} - (11.9i)c_4e^{(-11.9i)t} \tag{B55}$$

$$\dot{\phi} = 1.47(18.4i)c_1e^{(18.4i)t} - 1.47(18.4i)c_2e^{(-18.4i)t} + 1.15(11.9i)c_3e^{(11.9i)t} - 1.15(11.9i)c_4e^{(-11.9i)t} \tag{B56}$$

At $t = 0$, $\dot{\psi} = \dot{\phi} = 0$, so that equations (B55) and (B56) become

$$18.4c_1 - 18.4c_2 + 11.9c_3 - 11.9c_4 = 0 \tag{B57}$$

$$27.05c_1 - 27.05c_2 + 13.69c_3 - 13.69c_4 = 0 \tag{B58}$$

From equations (B53), (B54), (B57), and (B58),

$$\Delta = \begin{vmatrix} 1 & 1 & 1 & 1 \\ 1.47 & 1.47 & 1.15 & 1.15 \\ 18.4 & -18.4 & 11.9 & -11.9 \\ 27.05 & -27.05 & 13.69 & -13.69 \end{vmatrix} = -89.3 \tag{B59}$$

$$c_1 = \frac{\begin{vmatrix} \psi_o & 1 & 1 & 1 \\ \psi_o & 1.47 & 1.15 & 1.15 \\ 0 & -18.4 & 11.9 & -11.9 \\ 0 & -27.05 & 13.69 & -13.69 \end{vmatrix}}{-89.3} = -0.235\psi_o \tag{B60}$$

APPENDIX B

$$c_2 = \frac{\begin{vmatrix} 1 & \psi_o & 1 & 1 \\ 1.47 & \psi_o & 1.15 & 1.15 \\ 18.4 & 0 & 11.9 & -11.9 \\ 27.05 & 0 & 13.69 & -13.69 \end{vmatrix}}{-89.3} = -0.235\psi_o \tag{B61}$$

$$c_3 = \frac{\begin{vmatrix} 1 & 1 & \psi_o & 1 \\ 1.47 & 1.47 & \psi_o & 1.15 \\ 18.4 & -18.4 & 0 & -11.9 \\ 27.05 & -27.05 & 0 & -13.69 \end{vmatrix}}{-89.3} = 0.737\psi_o \tag{B62}$$

$$c_4 = \frac{\begin{vmatrix} 1 & 1 & 1 & \psi_o \\ 1.47 & 1.47 & 1.15 & \psi_o \\ 18.4 & -18.4 & 11.9 & 0 \\ 27.05 & -27.05 & 13.69 & 0 \end{vmatrix}}{-89.3} = 0.737\psi_o \tag{B63}$$

Substituting equations (B60) to (B63) into equations (B38) and (B51) results in

$$\psi = -0.235\psi_o e^{(18.4i)t} - 0.235\psi_o e^{(-18.4i)t} + 0.737\psi_o e^{(11.9i)t} + 0.737\psi_o e^{(-11.9i)t} \tag{B64}$$

$$\phi = 1.47(-0.235\psi_o)e^{(18.4i)t} + 1.47(-0.235\psi_o)e^{(-18.4i)t} + 1.15(0.737\psi_o)e^{(11.9i)t} + 1.15(0.737\psi_o)e^{(-11.9i)t} \tag{B65}$$

Since

$$\cos t = \frac{e^{it} + e^{-it}}{2} \tag{B66}$$

equations (B64) and (B65) become

$$\psi = -0.470\psi_o \cos (18.4t) + 1.474\psi_o \cos (11.9t) \tag{B67}$$

$$\phi = -0.691\psi_o \cos (18.4t) + 1.695\psi_o \cos (11.9t) \tag{B68}$$

The output torsion is

$$T_{||} = T_Y \cos \psi \cos (\phi - \psi) \tag{B69}$$

Equations (B67) and (B68) substituted in equation (B69) give

$$T_{||} = T_Y \cos \left[-0.470\psi_o \cos (18.4t) + 1.474\psi_o \cos (11.9t)\right] \times \cos \left[-0.221\psi_o \cos (18.4t) + 0.221\psi_o \cos (11.9t)\right] \tag{B70}$$

where

$$T_Y = K\theta \tag{B71}$$

Equation (B1), the differential equation for the perturbed condition, thus becomes

$$J\ddot{\theta} + \ell\dot{\theta} + K\theta \left\{\cos \left[-0.470\psi_o \cos (18.4t) + 1.474\psi_o \cos (11.9t)\right] \times \cos \left[-0.221\psi_o \cos (18.4t) + 0.221\psi_o \cos (11.9t)\right]\right\} = 0 \tag{B72}$$

Let

$$\cos \left[-0.470\psi_o \cos (18.4t) + 1.474\psi_o \cos (11.9t)\right] = \cos f(t) \tag{B73}$$

$$\cos \left[-0.221\psi_o \cos (18.4t) + 0.221\psi_o \cos (11.9t)\right] = \cos g(t) \tag{B74}$$

Thus, equation (B72), with the notation of the constants changed, becomes

$$\ddot{\theta} + 2c\omega\dot{\theta} + \omega^2\theta \cos f(t) \cos g(t) = 0 \tag{B75}$$

where $c = \ell/2J\omega$ and $\omega = \sqrt{K/J}$.

APPENDIX B

The modulation frequency is slow relative to the oscillating frequency; therefore, under these conditions, the Wentzel, Kramers, Brillouin (WKB) method of solution (from ref. 8) can be applied to solve equation (B75). Assume that

$$\theta = A(t)\, e^{i\beta(t)} \tag{B76}$$

Then

$$\dot{\theta} = Ai\dot{\beta}e^{i\beta} + \dot{A}e^{i\beta} \tag{B77}$$

$$\ddot{\theta} = Ai\dot{\beta}(i\dot{\beta})e^{i\beta} + Ae^{i\beta}i\ddot{\beta} + \dot{A}i\dot{\beta}e^{i\beta} + \dot{A}i\dot{\beta}e^{i\beta} + \ddot{A}e^{i\beta} \tag{B78}$$

Substituting equations (B76) to (B78) into equation (B75) gives

$$\ddot{A} + i(A\ddot{\beta} + 2\dot{A}\dot{\beta} - 2ic\omega\dot{A}) + A\left[\omega^2 \cos f(t) \cos g(t) - \dot{\beta}^2 + 2ic\omega\dot{\beta}\right] = 0 \tag{B79}$$

The expression in brackets in equation (B79) is arbitrarily set equal to zero:

$$\dot{\beta}^2 - 2ic\omega\dot{\beta} - \omega^2 \cos f(t) \cos g(t) = 0 \tag{B80}$$

Let

$$\left.\begin{aligned} F(t) &= \omega^2 \cos f(t) \cos g(t) \\ a &= 2c\omega \end{aligned}\right\} \tag{B81}$$

With equations (B81) substituted in equation (B80),

$$\dot{\beta}^2 - ia\dot{\beta} - F(t) = 0 \tag{B82}$$

$$\dot{\beta} = \frac{ia}{2} \pm \sqrt{-\frac{a^2}{4} + F(t)} \tag{B83}$$

Since A is slowly varying, $\dot{A}$ still slower, and $\ddot{A} \approx 0$, the following is obtained from equation (B79):

$$A\ddot{\beta} + \dot{A}(2\dot{\beta} - ia) = 0 \tag{B84}$$

APPENDIX B

$$A\ddot{\beta} + 2\dot{A}\left(\dot{\beta} - \frac{ia}{2}\right) = 0 \tag{B85}$$

$$\frac{\ddot{\beta}}{\dot{\beta} - \frac{ia}{2}} + \frac{2\dot{A}}{A} = 0 \tag{B86}$$

Integrating equation (B86) gives

$$\ln\left(\dot{\beta} - \frac{ia}{2}\right) + 2 \ln A = \ln c_5 \tag{B87}$$

$$A^2\left(\dot{\beta} - \frac{ia}{2}\right) = c_5 \tag{B88}$$

$$A = \pm c_5\left(\dot{\beta} - \frac{ia}{2}\right)^{-1/2} \tag{B89}$$

and substituting for $\dot{\beta}$ from equation (B83) gives

$$A = \pm c_5 \left\{\pm\left[-\frac{a^2}{4} + F(t)\right]^{1/2}\right\}^{-1/2} = \pm c_5 (\pm 1)^{1/2}\left[-\frac{a^2}{4} + F(t)\right]^{-1/4} \tag{B90}$$

Integrating equation (B83) gives

$$\beta = \frac{iat}{2} \pm \int \left[-\frac{a^2}{4} + F(t)\right]^{1/2} dt \tag{B91}$$

$$i\beta = -\frac{at}{2} \pm \int \left[-\frac{a^2}{4} + F(t)\right]^{1/2} dt$$

Substituting equations (B90) and (B91) in equation (B76) gives

$$\theta = \pm c_5 (\pm 1)^{1/2}\left[-\frac{a^2}{4} + F(t)\right]^{-1/4} \exp\left\{-\frac{at}{2} \pm i \int \left[-\frac{a^2}{4} + F(t)\right]^{1/2} dt\right\} \tag{B92}$$

Equation (B81) substituted in equation (B92) finally gives

$$\theta = \pm c_5 (\pm 1)^{1/2}\left[-(c\omega)^2 + \omega^2 \cos f(t) \cos g(t)\right]^{-1/4}$$

$$\times \exp\left\{-c\omega t \pm i \int \left[-(c\omega)^2 + \omega^2 \cos f(t) \cos g(t)\right]^{1/2} dt\right\} \tag{B93}$$

APPENDIX B

Note that the integral in equation (B93) may be written as

$$\pm i\omega \int \left[-c + \cos f(t) \cos g(t)\right]^{1/2} dt.$$

Refer to equations (B73) and (B74) and let

$$\alpha_1 = -0.470\psi_o \cos (18.4t)$$

$$\alpha_2 = 1.474\psi_o \cos (11.9t)$$

$$\beta_1 = -0.221\psi_o \cos (18.4t)$$

$$\beta_2 = 0.221\psi_o \cos (11.9t)$$

and let $\gamma = 18.4t$ and $\varepsilon = 11.9t$. Then

$$\cos f(t) \cos g(t) = \cos (\alpha_1 + \alpha_2) \cos (\beta_1 + \beta_2) \tag{B94}$$

and by series expansion,

$$\begin{aligned}\cos f(t) \cos g(t) = 1 &- \frac{1}{2}\left(\alpha_1^2 + 2\alpha_1\alpha_2 + \alpha_2^2 + \beta_1^2 + 2\beta_1\beta_2 + \beta_2^2\right) \\ &+ \frac{1}{4}\left(\alpha_1^2\beta_1^2 + 2\alpha_2^2\beta_1\beta_2 + \alpha_1^2\beta_2^2 + 2\alpha_1\alpha_2\beta_1^2\right. \\ &+ 4\alpha_1\alpha_2\beta_1\beta_2 + 2\alpha_1\alpha_2\beta_2^2 \\ &\left. + \alpha_2^2\beta_1^2 + 2\alpha_2^2\beta_1\beta_2 + \alpha_2^2\beta_2^2\right) + \ldots\end{aligned} \tag{B95}$$

Since ψ_o is a small angle, the small angle approximation can be made and all terms higher than second order can be eliminated. This finally gives

APPENDIX B

$$\cos f(t) \cos g(t) = 1 - 0.0675\psi_o^2 \cos 2\gamma - 0.0675\psi_o^2 + 0.742\psi_o^2 \cos\gamma \cos\varepsilon$$

$$- 0.555\psi_o^2 \cos 2\varepsilon - 0.555\psi_o^2 + 0.000338\psi_o^4 \cos 4\gamma$$

$$+ 0.000338\psi_o^4 + 0.00135\psi_o^4 \cos 2\gamma + 0.00135\psi_o^4$$

$$- 0.0700\psi_o^4 \cos 2\varepsilon \cos\varepsilon \cos\gamma - 0.0700\psi_o^4 \cos\varepsilon \cos\gamma$$

$$+ 0.0158\psi_o^4 \cos 2\gamma \cos 2\varepsilon + 0.0158\psi_o^4 \cos 2\gamma$$

$$+ 0.0158\psi_o^4 \cos 2\varepsilon + 0.0158\psi_o^4 + 0.00331\psi_o^4 \cos 4\varepsilon$$

$$+ 0.00331\psi_o^4 + 0.0132\psi_o^4 \cos 2\varepsilon + 0.00663\psi_o^4 \qquad \text{(B96)}$$

By gathering like cosine terms and taking ψ_o as a small angle, it can readily be seen that all terms containing ψ_o^4 can be dropped with little error. Then,

$$\cos f(t) \cos g(t) = 1 - 0.622\psi_o^2 - 0.0675\psi_o^2 \cos 2\gamma$$

$$- 0.555\psi_o^2 \cos 2\varepsilon + 0.742\psi_o^2 \cos\gamma \cos\varepsilon \qquad \text{(B97)}$$

and the integral in equation (B93) is

$$\pm i\omega \int \left[-c + 1 - 0.622\psi_o^2 - (0.0675 \cos 2\gamma + 0.555 \cos 2\varepsilon \right.$$

$$\left. - 0.742 \cos\gamma \cos\varepsilon)\psi_o^2\right]^{1/2} dt$$

Let $c_6 = -c + 1 - 0.622\psi_o^2$; then the integral becomes

$$\pm i\omega \int \left[c_6 - (0.0675 \cos 2\gamma + 0.555 \cos 2\varepsilon - 0.742 \cos\gamma \cos\varepsilon)\psi_o^2\right]^{1/2} dt$$

APPENDIX B

Expanding the integrand by the binomial expansion gives

$$\left[c_6 - (0.0675 \cos 2\gamma + 0.555 \cos 2\varepsilon - 0.742 \cos \gamma \cos \varepsilon)\psi_o^2\right]^{1/2}$$

$$= c_6^{1/2} - 1/2c_6^{-1/2}(0.0675 \cos 2\gamma + 0.555 \cos 2\varepsilon$$

$$- 0.742 \cos \gamma \cos \varepsilon)\psi_o^2 + \frac{1/2(-1/2)}{2} c_6^{-3/2}\left[(0.0675 \cos 2\gamma\right.$$

$$\left. + 0.555 \cos 2\varepsilon - 0.742 \cos \gamma \cos \varepsilon)\right]^2 \psi_o^4 + \ldots \quad \text{(B98)}$$

Again taking the small angle approximation for small ψ_o and discarding all terms higher than second order leaves the integral

$$\pm i\omega \int \left[c_6^{1/2} - \frac{\psi_o^2}{2c_6^{1/2}}(0.0675 \cos 2\gamma + 0.555 \cos 2\varepsilon - 0.742 \cos \gamma \cos \varepsilon)\right] dt \quad \text{(B99)}$$

Substituting $\gamma = 18.4t$ and $\varepsilon = 11.9t$ gives

$$\pm i\omega \int \left\{c_6^{1/2} - \frac{\psi_o^2}{2c_6^{1/2}}\left[0.0675 \cos 2(18.4t) + 0.555 \cos 2(11.9t)\right.\right.$$

$$\left.\left. - 0.742 \cos (18.4t) \cos (11.9t)\right]\right\} dt \quad \text{(B100)}$$

$$\pm i\omega\left(c_6^{1/2}t - \frac{\psi_o^2}{2c_6^{1/2}}\left\{0.0675\left[\frac{\sin 2(18.4t)}{2(18.4)}\right] + 0.555\left[\frac{\sin 2(11.9t)}{2(11.9)}\right]\right.\right.$$

$$\left.\left. - 0.742\left[\frac{\sin (18.4 - 11.9)t}{2(18.4 - 11.9)} + \frac{\sin (18.4 + 11.9)t}{2(18.4 + 11.9)}\right]\right\} + c_7\right) \quad \text{(B101)}$$

$$\pm i\omega\left(\left(1 - c - 0.622\psi_o^2\right)^{1/2}t - \frac{\psi_o^2}{2\left(1 - c - 0.622\psi_o^2\right)^{1/2}}\left\{\frac{0.0675}{18.4}\left[\frac{\sin 2(18.4t)}{2}\right]\right.\right.$$

$$\left.\left. + \frac{0.555}{11.9}\left[\frac{\sin 2(11.9t)}{2}\right] - 0.742\left[\frac{\sin (6.50t)}{13.0} + \frac{\sin (30.3t)}{60.6}\right]\right\} + c_7\right) \quad \text{(B102)}$$

Substituting the above for the integral expression in equation (B93) gives

$$\theta = \pm c_5(\pm 1)^{1/2}\left[-c^2\omega^2 + \omega^2 \cos f(t) \cos g(t)\right]^{-1/4}$$

$$\times \exp\left[-c\omega t \pm i\omega\left(\left(1 - c - 0.622\psi_o^2\right)^{1/2} t - \frac{\psi_o^2}{2\left(1 - c - 0.622\psi_o^2\right)^{1/2}}\right.\right.$$

$$\times \left\{0.00367\left[\frac{\sin 2(18.4t)}{2}\right] + 0.0466\left[\frac{\sin 2(11.9t)}{2}\right]\right.$$

$$\left.\left.\left. - 0.742\left[\frac{\sin (6.50t)}{13.0} + \frac{\sin (30.3t)}{60.6}\right]\right\} + c_7\right)\right] \qquad \text{(B103)}$$

Since ψ_o is a small angle, $\cos f(t) \cos g(t) \approx 1$ (see eq. (B97)) and the integrand remains real until the damping almost becomes critical and θ of equation (B93) is no longer valid since $\ddot{A} \neq 0$ in equation (B79). Normally, most torsional operation of this kind is sufficiently far away from critical damping operation to make equation (B93) quite valid. However, if the application is such that operation is close to critical, then there are computer programs which will solve equation (B75) by substituting

$$Z = \dot{\theta} \qquad \text{(B104)}$$

into equation (B75) and getting

$$\dot{Z} + 2c\omega Z + \omega^2\theta \cos f(t) \cos g(t) = 0 \qquad \text{(B105)}$$

Equations (B104) and (B105) are sufficient for the computer format.

The following is an outline of the procedure for obtaining a more general solution to the above problem. Since the above solution demonstrates that the perturbation does indeed produce a modulation on the output, it is sufficient for this paper. The more general solution is left for future development.

The angles ψ, ϕ, γ, and Ω shown in sketch (e) are the same or similar in sense to those used in spherical coordinates, and θ is the axial torsional angle. By convention, the Z-axis as shown should be negative but it is assumed positive.

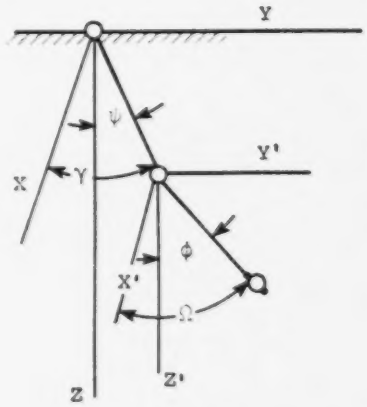

Sketch (e)

APPENDIX B

The coordinates of the center of gravity are

$$x = L_1 \sin\psi \cos\gamma + L_2 \sin\phi \cos\Omega \tag{B106}$$

$$y = L_1 \sin\psi \sin\gamma + L_2 \sin\phi \sin\Omega \tag{B107}$$

$$z = L_1 \cos\psi + L_2 \cos\phi \tag{B108}$$

The velocities are

$$\dot{x} = -L_1(\sin\psi)(\sin\gamma)\dot{\gamma} + L_1(\cos\gamma)(\cos\psi)\dot{\psi} - L_2(\sin\phi)(\sin\Omega)\dot{\Omega} + L_2(\cos\Omega)(\cos\phi)\dot{\phi} \tag{B109}$$

$$\dot{y} = L_1(\sin\psi)(\cos\gamma)\dot{\gamma} + L_1(\sin\gamma)(\cos\psi)\dot{\psi} + L_2(\sin\phi)(\cos\Omega)\dot{\Omega} + L_2(\sin\Omega)(\cos\phi)\dot{\phi} \tag{B110}$$

$$\dot{z} = -L_1(\sin\psi)\dot{\psi} - L_2(\sin\phi)\dot{\phi} \tag{B111}$$

The kinetic and potential energy become

$$T = \frac{m\dot{x}^2}{2} + \frac{m\dot{y}^2}{2} + \frac{m\dot{z}^2}{2} + \frac{I_\phi\dot{\phi}^2}{2} + \frac{I_\Omega\dot{\Omega}^2}{2} + \frac{I_\theta\dot{\theta}^2}{2} \tag{B112}$$

$$V = mg\left[L_1(1 - \cos\psi) + L_2(1 - \cos\phi)\right] + \frac{K}{2}(\theta^2 + \gamma^2 + \Omega^2) \tag{B113}$$

The Lagrangian then is

$$\mathfrak{L} = T - V = \frac{m}{2}\left[-L_1(\sin\psi)(\sin\gamma)\dot{\gamma} + L_1(\cos\gamma)(\cos\psi)\dot{\psi} - L_2(\sin\phi)(\sin\Omega)\dot{\Omega} + L_2(\cos\Omega)(\cos\phi)\dot{\phi}\right]^2 + \frac{m}{2}\left[L_1(\sin\psi)(\cos\gamma)\dot{\gamma} + L_1(\sin\gamma)(\cos\psi)\dot{\psi} + L_2(\sin\phi)(\cos\Omega)\dot{\Omega} + L_2(\sin\Omega)(\sin\phi)\dot{\phi}\right]^2 + \frac{m}{2}\left[-L_1(\sin\psi)\dot{\psi} - L_2(\sin\phi)\dot{\phi}\right]^2 + \frac{I_\theta\dot{\theta}^2}{2} + \frac{I_\phi\dot{\phi}^2}{2} + \frac{I_\Omega\dot{\Omega}^2}{2} - mgL_1(1 - \cos\psi) - mgL_2(1 - \cos\phi) - \frac{K}{2}(\theta^2 + \gamma^2 + \Omega^2) \tag{B114}$$

where

$$I_{\Omega} = I_{\phi} \tag{B115}$$

and where interactions and other effects might slightly alter θ, the output amplitude due to axial torsion, but most of the axial torque is assumed transmitted at all angles of the suspension (flexible rotary cable principle) from its normal. The upper and lower ends of the fiber suspensions are turned through angles γ and Ω by the normal torque component.

There are five generalized coordinates - ψ, ϕ, γ, Ω, and θ - represented by q_r and dissipative generalized forces due to damping. According to Lagrange's equation, namely,

$$\frac{d}{dt}\left(\frac{\partial \mathcal{L}}{\partial \dot{q}_r}\right) - \frac{\partial \mathcal{L}}{\partial q_r} = \text{Generalized force} \tag{B116}$$

five equations of motion are obtained which can be solved, as was done in this paper, for the output with perturbation effects.

APPENDIX C

DERIVATION OF DAMPING COEFFICIENT FROM A DECAY CURVE USING THE AXIS OF SYMMETRY AS THE REFERENCE DATUM

In this appendix, the equations for damping coefficient c and rigidity K are derived. To apply these equations, only two peak torsional amplitudes (measured from the axis of symmetry of the decay curve) and the number of half-periods between them must be known.

The equation for an unperturbed, freely oscillating torsion pendulum is

$$J\ddot{\theta} + \ell\dot{\theta} + K\theta = 0 \tag{C1}$$

where J is the polar torsional moment of inertia, ℓ is the damping constant, K is torsional rigidity, and θ, $\dot{\theta}$, and $\ddot{\theta}$ are the angular displacement, velocity, and acceleration of the pendulum. Let

$$b = \frac{\ell}{2J} \tag{C2}$$

and

$$\omega = \sqrt{\frac{K}{J}} \tag{C3}$$

Then equation (C1) becomes

$$\ddot{\theta} + 2b\dot{\theta} + \omega^2\theta = 0 \tag{C4}$$

and the solution of equation (C4) is

$$\theta = c_1 \exp\left(-b + \sqrt{b^2 - \omega^2}\right)t + c_2 \exp\left(-b - \sqrt{b^2 - \omega^2}\right)t \tag{C5}$$

The initial conditions at $t = 0$ are

$$\theta = \theta_o \qquad \dot{\theta} = 0 \tag{C6}$$

With these initial conditions, the constants c_1 and c_2 can be obtained, so that equation (C5) becomes

$$\theta = \frac{\theta_o}{2} \exp(-bt)\left[\left(1 + \frac{b}{\sqrt{b^2 - \omega^2}}\right) \exp\left(\sqrt{b^2 - \omega^2}\, t\right) + \left(1 - \frac{b}{\sqrt{b^2 - \omega^2}}\right) \exp\left(-\sqrt{b^2 - \omega^2}\, t\right)\right] \tag{C7}$$

Of interest is the underdamped case when

$$b < \omega \qquad i\omega' = i\sqrt{\omega^2 - b^2} \tag{C8}$$

where ω' is the damped angular velocity. Equation (C7) becomes

$$\theta = \theta_o \exp(-bt)\left(\cos \omega' t + \frac{b}{\omega'} \sin \omega' t\right) \tag{C9}$$

When t equals the period of oscillation T,

$$\omega' T = 2\pi \tag{C10}$$

and from equations (C2), (C3), (C8), and (C10)

$$T = \frac{2\pi}{\left[\frac{K}{J} - \left(\frac{\ell}{2J}\right)^2\right]^{1/2}} \tag{C11}$$

Let

$$\frac{b}{\omega} = c = \frac{\ell}{2(KJ)^{1/2}} \qquad \text{(Critical damping occurs when } c = 1.0) \tag{C12}$$

With equation (C12) in equation (C8),

$$\omega' = (1 - c^2)^{1/2} \omega \tag{C13}$$

and from equations (C11) and (C2)

$$K = \frac{4\pi^2 J}{T^2} + c^2 \omega^2 J \tag{C14}$$

APPENDIX C

The phase angle δ is

$$\delta = \tan^{-1} \frac{\omega'}{b} \tag{C15}$$

Equations (C8), (C9), (C12), (C13), and (C15) give

$$\theta = \frac{\theta_o \exp(-c\omega t)}{(1 - c^2)^{1/2}} \sin(\omega' t + \delta) \tag{C16}$$

The phase angle does not affect the period.

A typically damped output, on an expanded time base, would look like figure 11. To obtain the value of c from this output, initial conditions must be taken at a time t when $\dot{\theta} = 0$. Hence, at any arbitrary peak displacement, a time reference $t = 0$ is taken to obtain from equation (C16),

$$\theta_i = \frac{\theta_o}{(1 - c^2)^{1/2}} \sin \delta \tag{C17}$$

At $t = \pi n/\omega'$, where n is the number of half-periods between θ_i and θ_n,

$$\theta_n = \frac{\theta_o}{(1 - c^2)^{1/2}} \exp\left(\frac{-c\omega\pi n}{\omega}\right) \sin \delta \tag{C18}$$

From equations (C17) and (C18),

$$\frac{\theta_i}{\theta_n} = \exp\left(\frac{c\omega}{\omega'} \pi n\right) \qquad (n = 0,1,2,\ldots) \tag{C19}$$

$$c \frac{\omega}{\omega'} = \frac{\ln(\theta_i/\theta_n)}{\pi n} = a \tag{C20}$$

Substituting equation (C13) results in

$$c = \frac{a}{\sqrt{1 + a^2}} \tag{C21}$$

APPENDIX C

For obtaining c, the damping coefficient of the material, K, its rigidity, and G, its shear modulus, only two peak points and the number of half-periods separating them are needed. Since the expression used for obtaining c (eq. (C19)) is the decay envelope of the peaks, if two alternate peaks are used, the algebraic sign of one of them must be reversed. Either way, the axis $\theta = 0$ must be accurately known; this is a great disadvantage. In appendix D, a three-successive-peak method is derived which does not have this drawback.

APPENDIX D

THREE-SUCCESSIVE-PEAK METHOD OF OBTAINING DAMPING COEFFICIENT FROM A DECAY CURVE USING ANY DATUM AS A REFERENCE

In appendic C, equations were derived for obtaining damping coefficient c with two peak amplitudes and the number of half-periods between them known. However, with this method the peak values must be measured from $\theta = 0$, the axis of symmetry of the decay curve. There are numerous other ways of obtaining c, some employing alternate peak measurements and others employing successive peak measurements. It is felt that three successive peak measurements are best from the point of view of accuracy. One of the reasons for this conclusion can be seen from the calibrate curve in figure 13. If three successive points

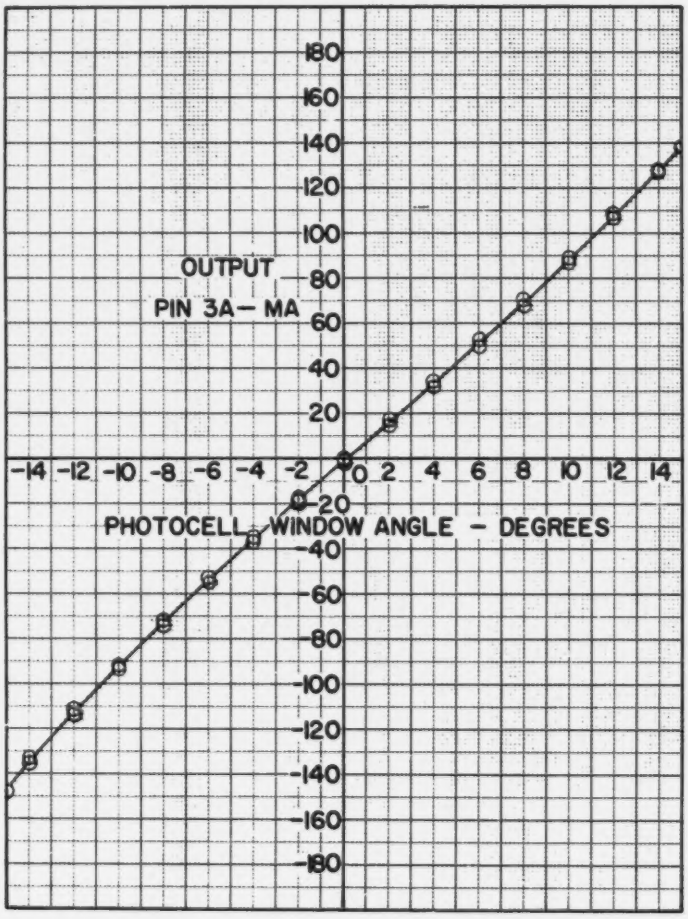

Figure 13.- Calibrate curve showing galvanometer output as a function of pendulum window angle input.

are taken, the effects of nonsymmetries, variations in sensitivity, and nonlinearity are either minimized or eliminated. In this appendix, the three-successive-peak method is derived; its only requirement is that the reference axis from which the three successive peak values are measured be parallel to $\theta = 0$. This is especially advantageous from the point of view of computer readout of data.

From equation (C18), θ for successive peaks is

$$\theta_n = \frac{\theta_o}{(1 - c^2)^{1/2}} \exp\left(- \frac{c\omega 2\pi n}{\omega'}\right) \sin \delta = \theta_o \exp\left(- \frac{c\omega 2\pi n}{\omega'}\right) \qquad (n = 0,1,2,\ldots) \qquad (D1)$$

where $\sin \delta = \omega'/\omega$ and $\omega' = (1 - c^2)^{1/2}\omega$. Also,

$$\theta_{n+1} = \theta_o \exp\left[- \frac{c\omega}{\omega'} 2\pi(n + 1)\right] \qquad (D2)$$

Consider the ratios of the general terms in equations (D1) and (D2):

$$\frac{\theta_n}{\theta_{n+1}} = \frac{\theta_o \exp\left(- \frac{c\omega}{\omega'} 2\pi n\right)}{\theta_o \exp\left[- \frac{c\omega}{\omega'} 2\pi(n + 1)\right]} = \exp\left(\frac{c\omega}{\omega'} 2\pi\right) = \text{Constant} \qquad (D3)$$

Now consider a translation of the θ,t coordinate system to the θ',t coordinate system, as shown in the following sketch:

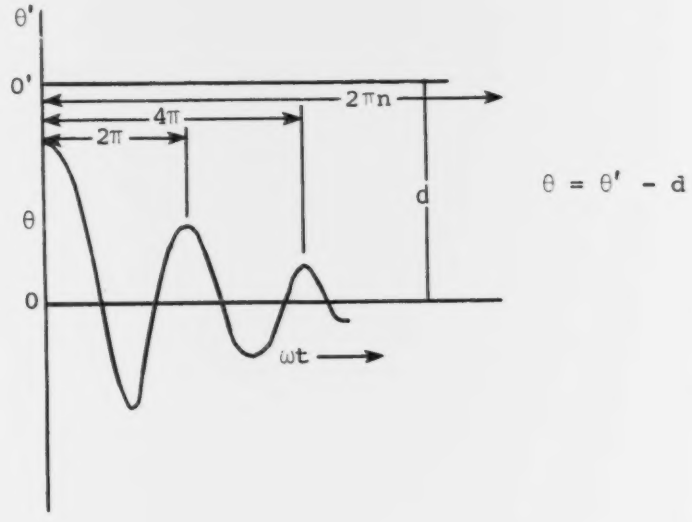

APPENDIX D

For this coordinate system

$$\theta'_n = \theta_n - d \qquad (n = 0,1,2,\ldots) \qquad \text{(D4)}$$

Substituting equation (D4) in equations (D1) and (D2) results in

$$\theta'_n + d = \theta_o \exp\left(-\frac{c\omega}{\omega'} 2\pi n\right) \qquad \text{(D5)}$$

$$\theta'_{n+1} + d = \theta_o \exp\left[-\frac{c\omega}{\omega'} 2\pi (n + 1)\right] \qquad \text{(D6)}$$

The ratio of equations (D5) and (D6) in the θ',t system is the same as in the θ,t system, that is,

$$\frac{\theta'_n + d}{\theta'_{n+1} + d} = \frac{\theta_o \exp\left(-\frac{c\omega}{\omega'} 2\pi n\right)}{\theta_o \exp\left[-\frac{c\omega}{\omega'} 2\pi (n + 1)\right]} = \exp\left(\frac{c\omega}{\omega'} 2\pi\right) = \text{Constant} \qquad \text{(D7)}$$

This equation can be solved for c to result in the two-point method derived in appendix C. However it is dependent on d. To avoid measuring d in equation (D7), consider the next successive peak

$$\theta_{n+2} + d = \theta_o \exp\left[-\frac{c\omega}{\omega'} 2\pi (n + 2)\right]$$

$$\frac{\theta'_{n+1} + d}{\theta'_{n+2} + d} = \exp\left(\frac{c\omega}{\omega'} 2\pi\right) \qquad \text{(D8)}$$

From equations (D7) and (D8)

$$\theta'_n + d = \exp\left(\frac{c\omega}{\omega'} 2\pi\right)\left(\theta'_{n+1} + d\right) \qquad \text{(D9)}$$

$$\theta'_{n+1} + d = \exp\left(\frac{c\omega}{\omega'} 2\pi\right)\left(\theta'_{n+2} + d\right) \qquad \text{(D10)}$$

APPENDIX D

Subtract $\theta'_{n+1} + d$ from both sides of equation (D9) and $\theta'_{n+2} + d$ from both sides of equation (D10) to obtain

$$\theta'_n - \theta'_{n+1} = \left[\exp\left(\frac{c\omega}{\omega'} 2\pi\right) - 1\right]\left(\theta'_{n+1} + d\right) \tag{D11}$$

$$\theta'_{n+1} - \theta'_{n+2} = \left[\exp\left(\frac{c\omega}{\omega'} 2\pi\right) - 1\right]\left(\theta'_{n+2} + d\right) \tag{D12}$$

Taking the ratio of equations (D11) and (D12) and substituting equation (D8) result in

$$\frac{\theta'_n - \theta'_{n+1}}{\theta'_{n+1} - \theta'_{n+2}} = \frac{\theta'_{n+1} + d}{\theta'_{n+2} + d} = \exp\left(\frac{c\omega}{\omega'} 2\pi\right) \tag{D13}$$

For $n = 0$,

$$\frac{\theta'_0 - \theta'_1}{\theta'_1 - \theta'_2} = \exp\left(\frac{c\omega}{\omega'} 2\pi\right) \tag{D14}$$

Taking the logarithm of both sides of equation (D14) results in

$$\frac{c\omega}{\omega'} = \frac{\ln\left(\frac{\theta'_0 - \theta'_1}{\theta'_1 - \theta'_2}\right)}{2\pi} = a \tag{D15}$$

This is similar to equation (C20). Note that this method requires three points θ'_0, θ'_1, and θ'_2 measured from any reference axis parallel to $\theta = 0$. Since this method is independent of the position of $\theta' = 0$, it is very desirable. No restriction was placed on the θ values; thus, they are the measured values including their sign as measured from the reference datum. For these reasons, this method is used for obtaining a and, from equation (C21), c, the dynamic damping. Note that the above development for three successive peaks may be readily extended to n successive peaks. For alternate peaks, however, the sign of the alternate peaks has to be reversed so that they lie on the exponential curve. Hence, for three alternate peaks,

$$\frac{c\omega}{\omega'} = \frac{\ln\left(\frac{\theta'_n - \theta'_{n+1}}{\theta'_{n+1} + \theta'_{n+2}}\right)}{\pi} \tag{D16}$$

Again, the algebraic values of θ' including their sign are measured from the reference datum.

REFERENCES

1. Gillham, J. K.: Torsional Braid Analysis. Encyclopedia of Polymer Science and Technology, Volume 14, John Wiley & Sons, Inc., c.1971, pp. 76-90.

2. Gillham, John K.: Thermomechanical Properties of Polymers by Torsional Braid Analysis. Thermoanalysis of Fibers and Fiber-Forming Polymers, Robert F. Schwenker, Jr., ed., Appl. Polym. Symp. No. 2, Interscience Publ., 1966, pp. 45-58.

3. Gillham, John K.: A Semimicro Thermomechanical Technique for Characterizing Polymeric Materials: Torsional Braid Analysis. AIChE J., vol. 20, no. 6, Nov. 1974, pp. 1066-1078.

4. Dalal, S. K.; Carl, G. L.; Inge, A. T.; and Johnston, N. J.: Torsional Braid Analysis: Automated Analyzer and Data Acquisition/Reduction Using a Programmable Calculator. Paper presented at the American Chemical Society 167th National Meeting (Los Angeles, California), Apr. 6-11, 1974.

5. Carl, G. L.; Inge, A. T.; Johnston, N. J.; and Dalal, S. K.: Automated Data Acquisition and Reduction System for Torsional Braid Analyzer. NASA Tech Brief B75-10073, May 1975.

6. Bryant, E. L.: Noncontacting Method for Measuring Angular Deflection. U.S. Pat. 4,189,234, Feb. 19, 1980.

7. Wallmark, J. Torkel: A New Semiconductor Photocell Using Lateral Photoeffect. Proc. IRE, vol. 45, no. 4, Apr. 1957, pp. 474-483.

8. Schiff, Leonard I.: Quantum Mechanics, Second ed., McGraw-Hill Book Co., Inc., 1955.

1. Report No.	2. Government Accession No.	3. Recipient's Catalog No.
NASA TP-1840		

4. Title and Subtitle	5. Report Date
DESIGN AND ANALYSIS OF A TORSION BRAID PENDULUM DISPLACEMENT TRANSDUCER	June 1981
	6. Performing Organization Code 505-31-53-04
7. Author(s)	8. Performing Organization Report No.
Emanuel Rind and Emmett L. Bryant	L-14183
	10. Work Unit No.
9. Performing Organization Name and Address	
NASA Langley Research Center Hampton, VA 23665	11. Contract or Grant No.
	13. Type of Report and Period Covered
12. Sponsoring Agency Name and Address	Technical Paper
National Aeronautics and Space Administration Washington, DC 20546	14. Sponsoring Agency Code

15. Supplementary Notes

16. Abstract

The dynamic properties at various temperatures of braids impregnated with polymer can be measured by using the braid as the suspension of a torsion pendulum. This report describes the electronic and mechanical design of a torsional braid pendulum displacement transducer which is an advance in the state of the art. The transducer uses a unique optical design consisting of refracting quartz windows used in conjunction with a differential photocell to produce a null signal. The release mechanism for initiating free torsional oscillation of the pendulum has also been improved. Analysis of the precision and accuracy of the transducer indicated that the maximum relative error in measuring torsional amplitude was approximately 0.7 percent. A serious problem inherent in all instruments which use a torsional suspension was analyzed: misalignment of the physical and torsional axes of the torsional member which results in modulation of the amplitude of the free oscillation.

17. Key Words (Suggested by Author(s))	18. Distribution Statement
Torsional pendulums Error analysis Material dynamic properties Optical systems and instrumentation High-temperature properties	Unclassified - Unlimited Subject Category 35

19. Security Classif. (of this report)	20. Security Classif. (of this page)	21. No. of Pages	22. Price
Unclassified	Unclassified	61	A04

For sale by the National Technical Information Service, Springfield, Virginia 22161

NASA-Langley, 1981